and endothelial progenitor cells (Rafii and Lyden, 2003). hUCB contains 10-times more $CD34^+$ mononuclear cells (MNCs) than does adult peripheral blood (Murohara et al., 2000). The proportion of $CD34^+$ cells in hUCB ranges from 0.3% (Sun et al., 2010) to 2.4% (de Paula et al., 2012), which is comparable to bone marrow (Cox et al., 2011). Because of this feature, hUCB has been used for hematopoietic stem cell transplantation in patients with hematological diseases and inherited metabolic disorders/neurodegenerative diseases, i.e., Hurler's syndrome, adrenoleukodystrophy, and Krabbe disease (Prasad et al., 2008). Apart from their hematopoietic properties, hUCB cells (hUCBCs) have myriad effects. Human $CD34^+$ cells secrete numerous cytokines, chemokines, and growth factors, including vascular endothelial growth factor (VEGF) (Majka et al., 2001). $CD34^+$ cells are less prevalent in the neonatal peripheral blood immediately after birth than in UCB and tend to decrease within the first 48 h after delivery (Kim et al., 2007). The basic concept underlying the intravenous administration of autologous UCBCs for NE is to replenish the reduced stem cells in systemic circulation, which may contribute to neuroprotection and/or enhance cerebral plasticity.

There are several dozen reports in the literature that have examined the effects of cell therapies in animal models of NE. Several cell types have been investigated (Chicha et al., 2014), including neural stem cells (Comi et al., 2008; Sato et al., 2008), MSCs (van Velthoven et al., 2010), multipotent adult progenitor cells (Yasuhara et al., 2006), and dental pulp-derived stem cells (Yamagata et al., 2013). Several cell sources have been investigated as well, i.e., rodent embryo (Comi et al., 2008; Sato et al., 2008), rodent or human bone marrow (Yasuhara et al., 2006; van Velthoven et al., 2010), and hUCB (Meier et al., 2006). Furthermore, several administration routes have also been investigated, i.e., intracerebral (Xia et al., 2010), intraperitoneal (Meier et al., 2006), and intranasal delivery (van Velthoven et al., 2013). Many studies have shown the benefits of cell therapy. Among these different cell therapies, the intravenous administration of autologous UCB treatment may have the lowest risk for clinical use in NE (Bennet et al., 2012). A few clinical trials using an intravenous administration of autologous UCB for NE are currently in progress (http://www.clinicaltrials.gov/, NCT00593242, NCT01506258, NCT01649648). However, little is known about the optimal protocol and the mechanisms of action of UCBC treatment. To date, there have been 15 reports in the literature examining the effects of UCBC treatment in rodent models of NE. These studies used either whole of the MNC fraction (Meier et al., 2006; de Paula et al., 2009, 2012; Pimentel-Coelho et al., 2010; Rosenkranz et al., 2010, 2012, 2013; Yasuhara et al., 2010; Geißler et al., 2011; Bae et al., 2012; Dalous et al., 2012; Wasielewski et al., 2012; Wang et al., 2013) or MSCs derived from hUCB (Xia et al., 2010; Kim et al., 2012). The effects of other cell populations in UCB for NE remain unknown. In this study, we focused on the $CD34^+$ cell fraction of hUCB. We have previously reported the beneficial effects of the systemic administration of hUCB-$CD34^+$ cells in an adult mouse model of stroke (Taguchi et al., 2004a). The objective of this study was to examine the effects of the intravenous administration of hUCB-$CD34^+$ cells on post-stroke recovery in a mouse model of neonatal stroke.

EXPERIMENTAL PROCEDURES

Animals and surgery

All experiments were performed in accordance with the NIH Guide for the Care and Use of Laboratory Animals and were approved by the Experimental Animal Care and Use Committee of the National Cerebral and Cardiovascular Center.

Ninety-one postnatal day 12 (P12) male and female mouse pups with severe combined immunodeficiency (SCID) (CB-17/Icr-scid/scidJcl; CLEA Japan Inc., Tokyo, Japan) were prepared for the experiments. P8–12 mice are considered comparable to human full-term (P0) neonates with regard to brain maturation (Hagberg et al., 2002); some authors argue that P12 mice are more representative of human full-term neonates (Charriaut-Marlangue et al., 2013). The novel model of neonatal stroke that we recently reported (Tsuji et al., 2013) uses CB-17 (CB-17/Icr-+/+Jcl) mouse pups, which are immunocompetent. As human cells were administered to mice, in the present study, we used immunocompromized animals to minimize immunological reactions due to xenotransplantation. The SCID mice used in the present study were derived from the same strain with the same genetic background as CB-17 mice. All efforts were made to minimize the number of animals used and their suffering.

Permanent middle cerebral artery occlusion (MCAO) was produced according to previously reported methods (Tsuji et al., 2013). Under isoflurane anesthesia (4.0% for induction and 1.5–2.0% for maintenance), a hole was made in the left temporal bone. The left middle cerebral artery (MCA) was electrocauterized and disconnected distal to crossing the olfactory tract. Thirteen pups underwent open-skull surgery without MCA electrocoagulation and served as sham-surgery controls. Five pups were excluded from the experimental analysis owing to bleeding during surgery. All analyses were performed by investigators who were blinded to the experimental group.

Cerebral blood flow (CBF) measurements

The cortical surface CBF was measured by a laser speckle flowmetry imaging system (Omegazone, Omegawave Inc., Tokyo, Japan) 24 h after MCAO, 24 h after treatment (i.e., 72 h after MCAO), and 1 and 7 weeks after treatment, as described previously, with one minor modification (Ohshima et al., 2012). We measured the CBF in two regions of interest (ROIs) through the intact skull with an open-scalp: the Core (the ischemic core region of the MCA territory) and the MCA region (the broader region covering most of the MCA territory, including the Core). The same grid was

used to set the two matching regions on the contralateral side. To analyze the influence of the treatment on the CBF in the peri-infarct regions, we measured the area in which the CBF was not attenuated, which we defined as the "well-perfused area." By observing the contralateral CBF visually, the area in which the CBF appeared equal to the corresponding contralateral side was manually demarcated using NIH Image software (ImageJ, 1.43r, NIH, Bethesda, MD, USA). For analytical accuracy of ROIs between animals and serial imaging, we set the ROI based on a line drawn from bregma to lambda, rather than basing it on the actual MCA-perfused territory. The percent of the well-perfused area was calculated by the ratio of the well-perfused area out of an area of a square grid, which primarily covered the MCA-perfused territory (Fig. 1A). All pups exhibited CBF reduction in the MCA territory after the MCAO. However, three mice exhibiting a mild CBF reduction, which was defined as a CBF ratio (ipsilateral/contralateral MCA region) > 0.80 at 24 h after MCAO, were removed from the study.

Administration of hUCB-CD34$^+$ cells after stroke

Seventy mice with MCAO were randomly assigned to one of two groups that received hUCB-CD34$^+$ cells (UCBC group) or phosphate-buffered saline (PBS group). Human UCB-CD34$^+$ cells were purchased from Lonza Inc. (Walkersville, MD, USA). The purity was >95%, and the viability of the cells was >95%. Forty-eight hours after the stroke, a skin incision was made under isoflurane anesthesia, and the left femoral vein was exposed. hUCB-CD34$^+$ cells (1×10^5 cells), or the same volume (40 μl) of PBS, were carefully infused into the femoral vein over 3 min using a 35G needle. We selected the dose of 1×10^5 hUCB-CD34$^+$ cells in the present study as the dose of 5×10^5 cells was beneficial in our previous study in an adult mouse model (Taguchi et al., 2004a). We selected the timing of cell administration at 48 h after the insult on the basis of our previous studies (Taguchi et al., 2004a; Uemura et al., 2012).

Behavioral tests

Rotarod and open-field tests were performed as described previously (Tsuji et al., 2013). Sensorimotor skills were evaluated 9 days and 7 weeks after the insult in the rotarod test. The rotarod accelerated from 4 to 40 rpm over 5 min (Muromachi Kikai Co., Ltd., Tokyo, Japan). The time until the mouse fell off the rotating drum was recorded for five consecutive sessions, and the average time spent on the drum was used for statistical comparison.

Locomotor and exploratory behaviors were evaluated 5 and 7 weeks after the insult using the open-field test.

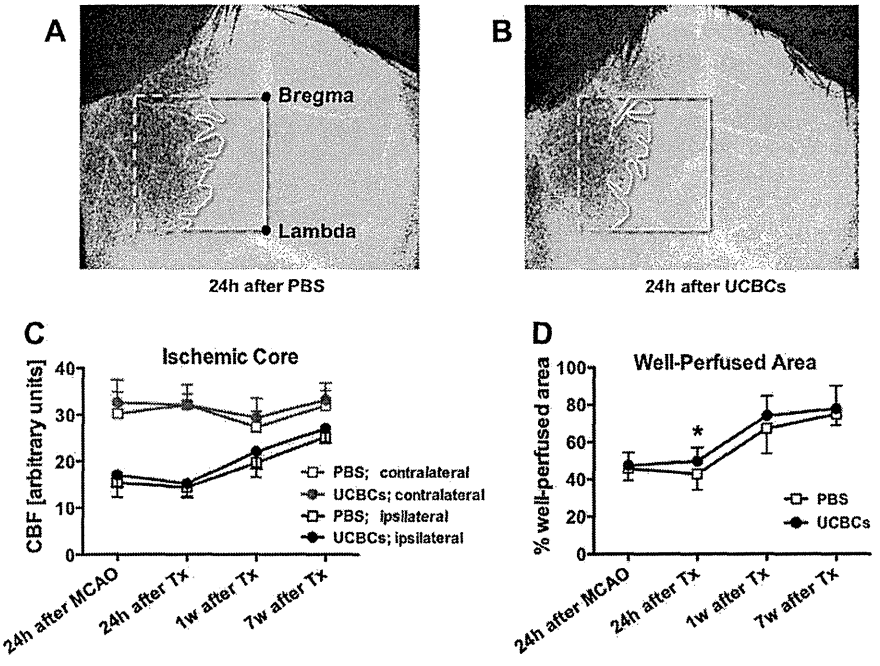

Fig. 1. Cerebral blood flow. (A, B) Representative images of the cerebral blood flow (CBF) 24 h after treatment (i.e., 72 h after the middle cerebral artery occlusion (MCAO)). The CBF was decreased in the MCA region on the ipsilateral side, which is indicated by the bluish color, after the MCAO insult. (C) There were no significant differences between the PBS-treated and human umbilical cord blood CD34$^+$ cell (UCBC)-treated groups with regard to CBF in the ischemic core. (D) However, with regard to the area of CBF reduction, there was a significant difference in the ratio of the area in which CBF was maintained (the area delineated by white lines in A, B) out of an area of a square (the square delineated by white dotted lines). The square was set based on a line drawn from bregma to lambda. We defined the ratio as the "% well-perfused area." Differences between groups were tested using a two-way repeated measures ANOVA. A post hoc test showed that the% well-perfused area was significantly larger in the UCBC group compared with the PBS group at 24 h after the treatment. *$P < 0.05$ (PBS-treated group n = 10–12 at each time point, except at 7 weeks after treatment (n = 5); UCBC-treated group n = 11–13 at each time point, except at 7 weeks after treatment (n = 4)). Tx; treatment.

Animals were allowed to search freely in a box (30 × 30 cm) for 30 min in a light environment and for the subsequent 30 min in a dark environment (Taiyo Electric Co., Ltd., Osaka, Japan). Infrared beams were mounted at specific intervals on the X-, Y-, and Z-banks of the open-field. The total number of beam crossings by the animal was counted and scored as "locomotion" for the horizontal movement and as "rearing" for the vertical movement.

Histological analyses

A morphological evaluation of the brain injury was performed as described previously (Tsuji et al., 2012, 2013). Animals were perfusion-fixed intracardially with 4% paraformaldehyde at 12 days or 7 weeks after the insult. The brain was removed and sectioned coronally in 1-mm-thick slices. The areas of the ipsilateral and contralateral hemispheres in each brain section were measured using ImageJ. The hemispheric volume was estimated by integrating the hemispheric areas. The % stroke volume was calculated as follows: ((contralateral volume – viable ipsilateral volume)/contralateral volume) × 100%. This model causes a pure cortical stroke with mild secondary injury in the thalamus and the corpus callosum, and the hemispheric volume effectively represents the histological injury (Tsuji et al., 2013).

Immunohistochemistry

Coronally sectioned brain slices were covered in tissue freezing medium (O.C.T. Compound, Sakura Finetek USA Inc., Torrance, CA, USA). Coronal sections (10 μm) were prepared using a cryostat (Leica Biosystems Inc., Wetzler, Germany). Sections were subjected to immunohistochemistry with anti-human nuclei antibody (HuNu) (Merck Millipore, Billerica, MA, USA, 1:30) and mouse-specific antibody to CD31 antigen expressed by endothelial cells (BD Biosciences, San Jose, CA, USA, 1:100); the secondary antibodies included anti-mouse Envision+ system-HRP Labeled Polymer and biotinylated anti-rat immunoglobulin (Dako Cytomation, Glostrup, Denmark), respectively. Nuclei were stained with hematoxylin after the HuNu staining. When analyzing the CD31-positive blood vessel, we defined the "peri-infarct area" as the external (non-ischemic) regions within 200 μm of the border of the post-stroke area, as described previously (Nakano-Doi et al., 2010). The lengths and diameters of blood vessels were measured using ImageJ.

Statistics

The mortality rate of the animals was analyzed using the Fisher's exact test. Differences in body weight were assessed using a one-way analysis of variance (ANOVA), followed by the Bonferroni test. The percent volume loss was assessed using a Student *t*-test. CBF, rotarod and open-field test outcomes were assessed using a two-way repeated measures ANOVA, followed by the Bonferroni test. Parameters in blood vessels were assessed using a two-way ANOVA, followed by the Bonferroni test. Differences were considered significant at $P < 0.05$. The results are expressed as the mean ± standard deviation (SD), unless otherwise noted.

RESULTS

Mortality and body weight

Mortality rates did not differ between the PBS and UCBC groups: 1 out of 35 mice in the PBS group and 2 out of 35 mice in the UCBC group. Body weights at the time of surgery (P12), and at 7 days (P21) and 7 weeks after the treatment (P63), did not differ among the three groups, including the sham-surgery control group (Table 1).

CBF

With regard to the degree of CBF reduction, there were no significant differences between the PBS and UCBC groups, either in the ischemic core (Fig. 1A–C) or in the MCA region (data not shown). However, with regard to the area of CBF reduction, a two-way repeated measures ANOVA showed that there was a significant group difference in the % well-perfused area: i.e., the areas where CBF was maintained were different (Fig. 1A, B, and D). A post hoc test showed that the % well-perfused area was significantly larger in the UCBC group compared with the PBS group at 24 h after the treatment, but not at the other time points measured.

Morphological brain injury

All pups subjected to MCAO exhibited cortical infarct and consistent hemispheric volume loss when assessed either 12 days or 7 weeks after the insult (Fig. 2A, B). Twelve days after MCAO, the mean % stroke volume did not differ between the PBS and UCBC groups, 20.7 ± 3.3% and 21.3 ± 2.4%, respectively (Fig. 2A). Seven weeks after MCAO, the mean% stroke volume in the UCBC group (21.5 ± 1.9%) was significantly ameliorated compared with the PBS group (25.6 ± 5.1%) (Fig. 2B–D). No sex differences in % stroke volume were observed in either of the groups (male 26.2 ± 3.9 vs. female 24.8 ± 6.5% in the PBS group, male 21.4 ± 1.2 vs. female 21.5 ± 2.3% in the UCBC group, at 7 weeks after MCAO).

Table 1. Body weights

	P12	P21	P63
Sham-surgery	6.9 ± 0.6	8.6 ± 0.5	20.0 ± 1.7
MCAO + PBS	6.7 ± 0.7	8.0 ± 0.7	18.2 ± 3.6
MCAO + UCBCs	6.7 ± 0.7	7.9 ± 0.7	18.2 ± 3.1

Body weights (g) (mean ± SD) at postnatal day 12 (P12, the day of surgery), P21 (7 days after the treatment), and P63 (7 weeks after the treatment) were not different between groups. MCAO, middle cerebral artery occlusion; PBS, phosphate-buffered saline; UCBCs, human umbilical cord blood $CD34^+$ cells.

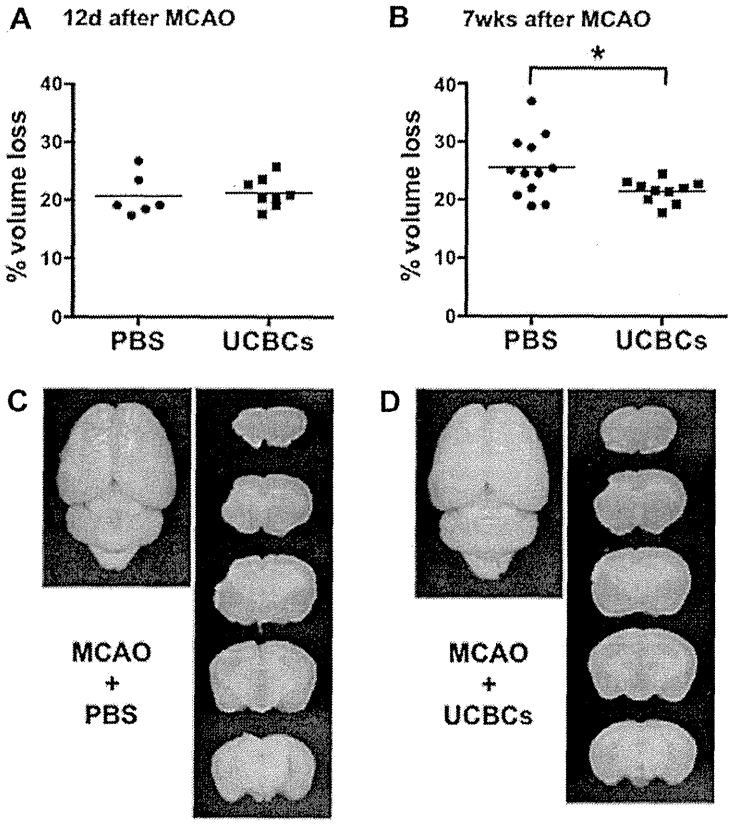

Fig. 2. Morphological brain injury. (A) Twelve days after middle cerebral artery occlusion (MCAO), the mean % stroke volume did not differ between the PBS-treated and human umbilical cord blood CD34$^+$ cell (UCBC)-treated groups. (B) Seven weeks after MCAO, the mean % stroke volume in the UCBC group was significantly ameliorated compared with the PBS group. (C) Representative images of brains 7 weeks after MCAO. *$P < 0.05$.

Localization of hUCB-CD34$^+$ cells

Very few donor cells stained with human antinuclear antibody were identified in the brain (a few stained cells per the entire coronal section) 24 h after the intravenous injection ($n = 5$), most of which were located around blood vessels (Fig. 3). The stained cells were hardly identified 10 days after the injection ($n = 5$) (data not shown).

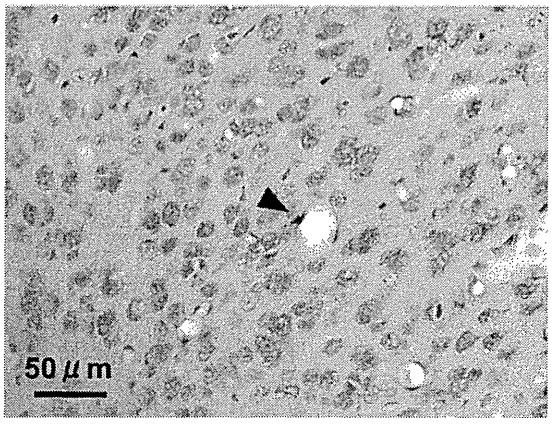

Fig. 3. Administered human umbilical cord blood CD34$^+$ cells. Very few donor cells, i.e., human umbilical cord blood CD34$^+$ cells stained with human antinuclear antibody, were identified in the brain 24 h after the intravenous injection. Donor cells that were identified were localized around blood vessels (arrowhead).

Blood vessels

We analyzed blood vessels in the region bordering the cortical infarct at 7 weeks after MCAO (Fig. 4A). There were no significant differences in either the number of vessels or the total length of vessels between the PBS and UCBC groups (Fig. 4B–E). However, the mean diameter of vessels was significantly larger in the UCBC-treated mice compared with the PBS-treated mice (Fig. 4B, C, and F). These large vessels in the UCBC-treated mice were observed only in the region bordering the cortical infarct and not in the other regions of the ipsilateral side or in the contralateral side.

Rotarod performance

Sensorimotor performance, as assessed by a rotarod treadmill at 9 days and 6 weeks after the insult, was analyzed by a two-way repeated measures ANOVA. There were significant group, but not time, differences. Compared with the performance in the sham-surgery group (238 ± 46 s, at 6 weeks), the performance was significantly impaired in mice with MCAO + PBS (175 ± 49 s), while no significant impairment was

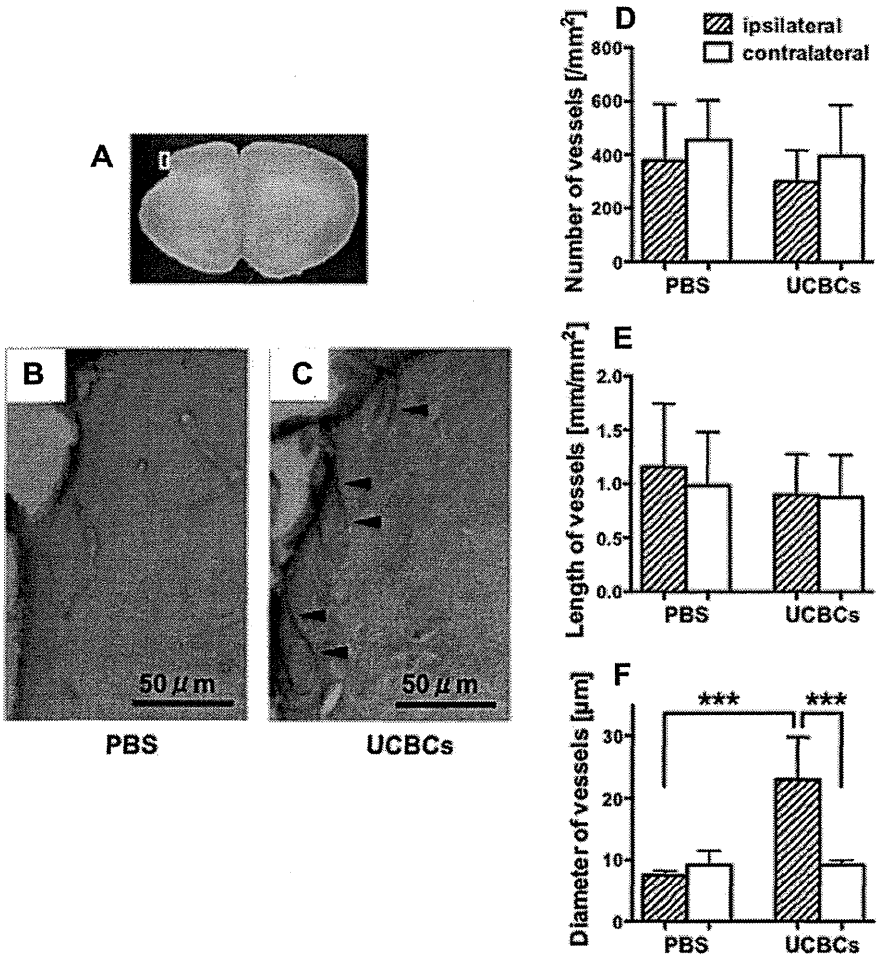

Fig. 4. Blood vessels. (A) Blood vessels in the peri-stroke region (small white square) were analyzed 7 weeks after MCAO. (B, C) Representative images of vessels stained with CD31 antibody (a marker of endothelial cells) in the peri-stroke regions. (D, E) There were no significant differences in either the number of vessels or the total length of vessels between the PBS-treated and human umbilical cord blood $CD34^+$ cell (UCBC)-treated groups. (F) However, the mean diameter of vessels in the peri-stroke region was significantly larger in the UCBC-treated mice compared with the PBS-treated mice. These large vessels in the UCBC-treated mice were only observed in the peri-stroke regions of the cortical infarct. ***$P < 0.001$.

observed in mice with MCAO + UCBCs (203 ± 54 s) (Fig. 5). However, there was no significant difference between the MCAO + UCBC group and the MCAO + PBS group. No sex differences in the performance were observed in either of the groups (male 188 ± 32 vs. female 155 ± 61 s in the PBS group, male 185 ± 43 vs. female 220 ± 57 s in the UCBC group, at 6 weeks).

Open-field activities

We initially analyzed the overall activities during 60-min sessions at 5 and 7 weeks after the insult using a two-way repeated measures ANOVA (data not shown). We then analyzed the temporal changes throughout a 60-min session in 5-min increments using a two-way repeated measures ANOVA (Fig. 6A, B). Compared with sham-surgery mice, mice with MCAO did not exhibit significant behavioral alterations in either locomotion or rearing at either time point; one exception

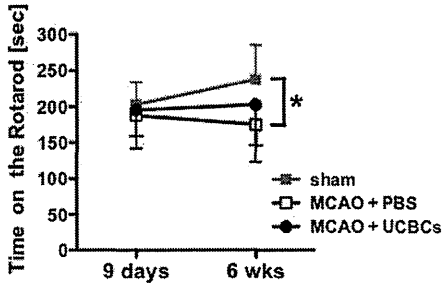

Fig. 5. Rotarod test. Repeated-measures two-way ANOVA showed significant group differences in sensorimotor performance. Performance was significantly impaired in mice with MCAO treated with PBS compared with sham-surgery mice. In contrast, performance was not impaired in mice with MCAO treated with human umbilical cord blood $CD34^+$ cells (UCBCs) compared with sham-surgery mice. However, there was no significant difference between the MCAO + UCBCs group and the MCAO + PBS group. *$P < 0.05$. (sham $n = 10$; MCAO + PBS $n = 12$; MCAO + UCBCs $n = 16$, 9 days after the insult, i.e., 1 week after the treatment. $n = 10$ in each group, 6 weeks after the insult).

was mice with MCAO treated with either PBS or UCBCs that exhibited significantly less prominent responses to the dark environment with respect to locomotion at both 5 and 7 weeks after the insult. Overall, UCBC treatment did not significantly alter the behaviors in the mice with neonatal stroke, as assessed with the open-field test.

DISCUSSION

Only two cell types, the whole MNC fraction and MSCs, in hUCB have been investigated as cell therapies in animal models of NE to date. In the present study, the intravenous administration of hUCB-CD34$^+$ cells, which are mostly hematopoietic stem cells and endothelial progenitor cells, modestly ameliorated histological brain injury after neonatal stroke in mice. The effects were, at least in part, due to the improved CBF in the ischemic penumbra during the subacute phase of stroke, which may be associated with the increased mean diameter of blood vessels observed in the peri-infarct area during the chronic phase.

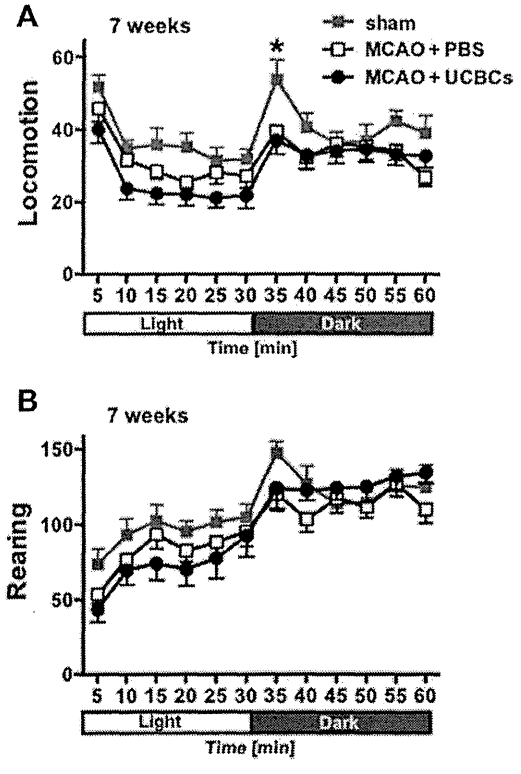

Fig. 6. Open-field test. Temporal changes in activities were analyzed in 5-min increments by a repeated-measures two-way ANOVA. (A) With respect to locomotion (horizontal movement), the mice in all three groups became hyperactive in response to the dark environment when assessed at 7 weeks after the insult. However, the response was significantly weaker in the mice with MCAO treated with either PBS or human umbilical cord blood CD34$^+$ cells (UCBCs) compared with the sham-surgery mice. (B) With respect to rearing (vertical movement), there were no significant group differences at 7 weeks after the insult. UCBC treatment did not significantly alter behavior in the mice with neonatal stroke. *$P < 0.05$ compared with the MCAO + PBS and MCAO + UCBCs groups. Mean ± SEM. (sham $n = 13$; MCAO + PBS $n = 17$; MCAO + UCBCs $n = 13$).

The purpose of the present study was to examine the potential of the CD34$^+$ cell fraction in human UCB; SCID mice, which are deficient in functional B and T lymphocytes because of a single gene mutation, were transfused with hUCB-CD34$^+$ cells. Hence, the present study used xenotransplantation; thus, caution should be exercised when translating the data obtained in the present study into the clinic. We used immunocompromized mice to minimize the undesirable immunological and inflammatory reactions caused by xenotransplantation as these reactions are not induced in autologous transfusion, which is the expected paradigm in the clinical application. To date, no study has examined the effects of allogeneic transplantation with UCBCs in rodent models of brain injury. One reason is because the rodent UCB is different from the human UCB; unlike in humans, mouse CD34$^+$ cells are not hematopoietic cells (Osawa et al., 1996). In addition, collecting rodent UCBCs is technically difficult.

We chose the timing of the cell transfusion to be 48 h after the brain injury for numerous reasons. The optimal time window of hUCBC therapies in animal models of NE has not been examined. UCBCs were administered 24 h after the brain injury in most NE studies (Table 2). Recent data on UCBCs and other types of stem cells in adult rodent models suggest that a later timing of transfusion, i.e., 48 or 72 h after the insult, is more beneficial (Newcomb et al., 2006; Rosenblum et al., 2012; Uemura et al., 2012).

One of the key features of this study is that it was performed using a highly reproducible model of NE, in which the locations of the infarct and peri-infarct areas were easily distinguishable and consistent between animals. During the first hours after brain injury, a detrimental biological cascade begins, and cells are destined to be damaged. We assumed that the neuroprotective effects would be limited when animals were treated 48 h after the insult, even if the cell treatment was potent. In fact, the hUCB-CD34$^+$ cell treatment achieved a modest, but statistically significant, amelioration of the brain injury. Similarly, the cell treatment exhibited a statistically significant augmentation of the CBF in the peri-infarct region, but not in other regions. These results suggest that the cell therapy exerts neuroprotective effects only in the peri-infarct area and not in the ischemic core. Moreover, these results suggest that it is crucial to examine the effects of treatment in a region-specific manner in a highly reproducible model.

The amelioration rate of cerebral tissue loss by the UCBC therapy was relatively small, and none of the UCBC-treated mice exhibited outstanding improvement; there may be a limit of the improvement in % stroke volume, e.g., 17.5% in this study. This implies that the ischemic core cannot be rescued or restored by cell treatment. The result is well conceivable as the model used in the present study is a permanent MCAO model in mice with a CB-17 strain background, which has little anastomoses between MCA and other cerebral arteries (Taguchi et al., 2010). Even after removing the pup with

Table 2. Reported studies with umbilical cord blood cells in rodent models of neonatal brain injury

Research group		Model	Cell type	Cell dose	Timing	Delivery route	Follow-up	Improvement		Author and reference
								Morphology	Behavior	
A	1	P7 rat, HI	MNC	1×10^7	24 h	i.p.	2 weeks	NA	+	Meier et al. (2006)
	2	P7 rat, HI	MNC	1×10^7	24 h	i.p.	2 weeks	NA	NA	Rosenkranz et al. (2010)
	3	P7 rat, HI	MNC	1×10^7	24 h	i.p.	6 weeks	NA	+	Geißler et al. (2011)
	4	P7 rat, HI	MNC	1×10^7	24 h	i.p., intrathecal	6 weeks	+	+	Wasielewski et al. (2012)
	5	P7 rat, HI	MNC	1×10^7	24 h	i.p.	2 weeks	+	NA	Rosenkranz et al. (2012)
	6	P7 rat, HI	MNC	1×10^7	24 h	i.p.	2 weeks	NA	NA	Rosenkranz et al. (2013)
B	7	P7 rat, HI	MNC	1×10^7	24 h	i.v.	3 weeks	–	–	de Paula et al. (2009)
	8	P7 rat, HI	MNC	1×10^6, 10^7, 10^8	24 h	i.v.	8 weeks	+	+	de Paula et al. (2012)
C	9	P7 rat, HI	MNC	1.5×10^4	7 days	i.v.	3 weeks	+	+	Yasuhara et al. (2010)
D	10	P7 rat, HI	MNC	2×10^6	3 h	i.p.	7 days	+	+	Pimentel-Coelho et al. (2010)
E	11	P7 rat, HI	MNC	$1 \times 1 \times 10^7$	24 h	i.v.	10 weeks	+	+	Bae et al. (2012)
F	12	P5 rat, excitotoxicity	MNC	1, 3×10^6, 1×10^7	0, 24 h	i.p., i.v.	5 days	–	NA	Dalous et al. (2012)
G	13	P7 rat, HI	MNC	3×10^6	24 h	Intraventricular	2 weeks	+	NA	Wang et al. (2013)
H	14	P7 rat, HI	MSC	5×10^4	3 days	Intraparenchymal	4 weeks	+	+	Xia et al. (2010)
I	15	P10 rat, MCAO	MSC	1×10^5	6 h	Intraventricular	4 weeks	+	+	Kim et al. (2012)
Present study		P12 mouse, MCAO	$CD34^+$ cell	1×10^5	48 h	i.v.	7 weeks	+	–	

P, postnatal day; HI, hypoxia–ischemia; MCAO, middle cerebral artery occlusion; MNC, mononuclear cell; MSC, mesenchymal stem cell; i.p., intraperitoneal; i.v., intravenous; NA, not assessed.

the most severe brain damage in the PBS group, the ameliorating effects of the cell therapy were statistically significant, confirming the fact that the treatment effect is modest but significant.

$CD34^+$ cells as a neuroprotective treatment

The intravenous administration of hUCB-$CD34^+$, but not $CD34^-$ cells, ameliorates damage in adult mice with permanent MCAO (Taguchi et al., 2004a) and in a rat model of spinal cord injury (Kao et al., 2008). Boltze et al. (2012) compared the effects of the intravenous administration of hUCB-MNCs (which contains a variety of cells, including $CD34^+$ cells), $CD34^+$ cells, and $CD34^-$ cells in adult rats with permanent MCAO. The MNCs provided the most prominent neuroprotective effects, with $CD34^+$ cells appearing to be particularly involved in the protective action of MNCs. A study in a rat model of myocardial infarction showed that $CD34^+$ cell treatment elicited the greatest attenuation of the damage with the high-dose MNC group (which contained the same absolute $CD34^+$ cell dose as the $CD34^+$ cell group) exhibiting a moderate attenuation (Kawamoto et al., 2006). The beneficial effects of the intravenous administration of hUCB-$CD34^+$ cells have also been reported in adult rat models of transient MCAO (Chen et al., 2001; Ou et al., 2010), heatstroke (Chen et al., 2007) and traumatic brain injury (Chen et al., 2013). Among the variety of cell types in hUCB, $CD34^+$ cells play a crucial, if not absolute, role in the neuroprotection afforded by hUCBC treatment. In our clinical studies of adult patients with cerebral ischemic events, the number of circulating $CD34^+$ cells was inversely correlated with cerebral infarction and positively correlated with CBF (Taguchi et al., 2004b, 2009). These results suggest that circulating $CD34^+$ cells have a role in the maintenance of the cerebral circulation in ischemic stress.

The administration of whole nucleated cells or the MNC fraction isolated by a density gradient separation is a simple approach for clinical application. Of note, the "MNC fraction" does not necessarily indicate that the cells in the fraction are exclusively mononucleate cells. The hUCB-MNC fraction isolated by gradient separation using Ficoll-paque (GE Healthcare UK Ltd., Amersham Place, England) contains 1–20% granulocytes among the recovered cells. As much as 46% of the MNC fraction is composed of granulocytes after separation from child bone marrow (Cox et al., 2011). As some studies have shown that granulocytes are detrimental for NE (Palmer et al., 2004), the administration of only the beneficial cell fraction may be important to improve the clinical outcome.

Augmentation of CBF and modulation of blood vessels by UCBC treatment

The present study shows that augmentation of CBF is one of the beneficial effects of hUCB-$CD34^+$ cell treatment. Our previous study demonstrated that the degree of CBF reduction in the subacute phase following neonatal HI (24 h after the insult) correlated strongly with the

subsequent morphological development of brain damage in mice (Ohshima et al., 2012). This implies that augmentation of the CBF during this phase may lead to improvements in brain damage during the chronic phase. We have previously reported that the intravenous administration of hUCB-CD34$^+$ cells enhanced CBF just outside of the penumbra in an adult mouse model of permanent MCAO (Taguchi et al., 2004a). We have reported that the intravenous administration of murine bone marrow MNCs markedly augmented CBF in the early phase after treatment (6 h after administration) in an adult mouse model of ischemic white matter damage (Fujita et al., 2010). Augmentation of CBF induced by CD34$^+$ cell treatment has also been reported in adult rat models of transient three-vessel-occlusion (Shyu et al., 2006) and heatstroke (Chen et al., 2007).

In the present study, we found that the cell therapy can modulate the morphologies of blood vessels after an ischemic insult, i.e., an enlarged diameter of blood vessels. We have previously reported that cell therapies can modulate the morphologies of blood vessels after ischemic insults, leading to an increased density of blood vessels in the adult models (Taguchi et al., 2004a; Fujita et al., 2010). Angiogenesis facilitated by CD34$^+$ cell treatment has also been reported in other models of brain injury (Shyu et al., 2006; Chen et al., 2007, 2013) and myocardial infarction (Kawamoto et al., 2006). In the present study, there was no accumulation of hUCB-CD34$^+$ cells in the border area of the infarct; the number of donor cells in the brain was substantially lower at 24 h after administration, and the donor cells were virtually absent by 10 days after administration. Therefore, it is highly unlikely that the donor cells contributed physically to the enlargement of the blood vessels after their incorporation. Although we previously identified that a few donor cells reside in the vascular walls and express endothelial markers or features of pericytes, this is not a prevalent phenomenon in the ischemic brain (Taguchi et al., 2004a; Fujita et al., 2010). A body of evidence demonstrates the beneficial effects of cell therapies in animal models of brain injury in the absence (Borlongan et al., 2004; Boltze et al., 2012) or paucity (Yasuhara et al., 2010) of hUCBCs in brain tissue.

There have been no studies that directly examined angiogenesis after hUCBC treatment in animal models of NE. However, one study demonstrated a possible association between hUCBC treatment and angiogenesis in an animal model of NE. The study showed that an intraperitoneal application of hUCB-MNCs increased the expression of the proteins Tie-2, occludin, and VEGF in the brain, which are associated with angiogenesis (Rosenkranz et al., 2012). Increased levels of VEGF in the central nervous system following the intravenous administration of hUCB-CD34$^+$ cells have been reported in an adult rat model of spinal cord injury (Kao et al., 2008). Increases in endothelial nitric oxide synthase activation by bone marrow-MNC treatment have been observed in ischemic brains (Fujita et al., 2010). We suggest that the direct structural incorporation of donor cells within blood vessels may not be the main mechanism underlying the modulation of CBF and blood vessels but rather VEGF, nitric oxide, or unknown factors that are induced by cell treatment are responsible.

Other effects of UCBC treatment

Apart from its effects on CBF and blood vessels, the pluripotent nature of hUCBC treatment has been reported to be one of the mechanisms responsible for the beneficial effects of this treatment for NE (Verina et al., 2013). Although there are no reports of the use of hUCB-CD34$^+$ cells in NE, there are 15 reports of the use of other types of hUCBCs (Table 2). Systemic (i.e., intraperitoneal or intravenous) injection of hUCB-MNCs in a neonatal rat model of HIE reduced apoptosis (Pimentel-Coelho et al., 2010; Rosenkranz et al., 2012); increased the expression of brain-derived neurotrophic factor (BDNF) (Rosenkranz et al., 2012), nerve growth factor, and glial cell line-derived neurotrophic factor (GDNF) in the brain (Yasuhara et al., 2010); reduced the activation of astrocytes (Wasielewski et al., 2012) and microglia (Pimentel-Coelho et al., 2010; Rosenkranz et al., 2013); reduced the increase in serum levels of pro-inflammatory cytokines (Rosenkranz et al., 2013); and restored neural processing in the primary somatosensory cortex (Geißler et al., 2011). Studies in adult rodent models of CNS disorders have shown that hUCB-CD34$^+$ cell treatment increased brain levels of trophic factors, i.e., GDNF, and decreased serum levels of systemic inflammatory molecules, i.e., tumor necrosis factor-α and intercellular adhesion molecule-1 (Chen et al., 2007, 2013; Kao et al., 2008; Ou et al., 2010).

Taken together, the major mechanisms responsible for the beneficial effects of hUCB treatment for cerebral ischemia appear to be related to either immunomodulation/anti-inflammation and/or trophic factor/cytokine production, independently of CBF/blood vessel modulation. Our present study suggests that the modulation of these immuno-inflammatory responses is not the single mechanism of action of hUCBC treatment, as SCID mice (which lack both functional T and B lymphocytes) exhibited improvement after cell therapy.

CONCLUSIONS

This study shows that the intravenous administration of hUCB-CD34$^+$ cells 48 h after neonatal stroke modestly ameliorates brain injury in a mouse model.

Acknowledgments—We thank Manami Sone and Mari Furuta for excellent technical assistance. We also thank Kenichi Mishima, Ph.D. for helpful discussions. This work was supported by JSPS KAKENHI Grant Number 24591617.

REFERENCES

Bae SH, Kong TH, Lee HS, Kim KS, Hong KS, Chopp M, Kang MS, Moon J (2012) Long-lasting paracrine effects of human cord blood cells on damaged neocortex in an animal model of cerebral palsy. Cell Transplant 21:2497–2515.

Bennet L, Tan S, Van den Heuij L, Derrick M, Groenendaal F, van Bel F, Juul S, Back SA, Northington F, Robertson NJ, Mallard C, Gunn AJ (2012) Cell therapy for neonatal hypoxia–ischemia and cerebral palsy. Ann Neurol 71:589–600.

Boltze J, Reich DM, Hau S, Reymann KG, Strassburger M, Lobsien D, Wagner DC, Kamprad M, Stahl T (2012) Assessment of neuroprotective effects of human umbilical cord blood mononuclear cell subpopulations in vitro and in vivo. Cell Transplant 21:723–737.

Borlongan CV, Hadman M, Sanberg CD, Sanberg PR (2004) Central nervous system entry of peripherally injected umbilical cord blood cells is not required for neuroprotection in stroke. Stroke 35:2385–2389.

Chabrier S, Husson B, Dinomais M, Landrieu P, Nguyen The Tich S (2011) New insights (and new interrogations) in perinatal arterial ischemic stroke. Thromb Res 127:13–22.

Charriaut-Marlangue C, Bonnin P, Leger PL, Renolleau S (2013) Brief update on hemodynamic responses in animal models of neonatal stroke and hypoxia–ischemia. Exp Neurol 248:316–320.

Chen J, Sanberg PR, Li Y, Wang L, Lu M, Willing AE, Sanchez-Ramos J, Chopp M (2001) Intravenous administration of human umbilical cord blood reduces behavioral deficits after stroke in rats. Stroke 32:2682–2688.

Chen SH, Chang FM, Chang HK, Chen WC, Huang KF, Lin MT (2007) Human umbilical cord blood-derived CD34$^+$ cells cause attenuation of multiorgan dysfunction during experimental heatstroke. Shock 27:663–671.

Chen SH, Wang JJ, Chen CH, Chang HK, Lin MT, Chang FM, Chio CC (2013) Umbilical cord blood-derived CD34$^+$ cells improve outcomes of traumatic brain injury in rats by stimulating angiogenesis and neurogenesis. Cell Transplant. http://dx.doi.org/10.3727/096368913X667006.

Chicha L, Smith T, Guzman R (2014) Stem cells for brain repair in neonatal hypoxia–ischemia. Childs Nerv Syst 30:37–46. http://dx.doi.org/10.1007/s00381-013-2304-4.

Comi AM, Cho E, Mulholland JD, Hooper A, Li Q, Qu Y, Gary DS, McDonald JW, Johnston MV (2008) Neural stem cells reduce brain injury after unilateral carotid ligation. Pediatr Neurol 38: 86–92.

Cox Jr CS, Baumgartner JE, Harting MT, Worth LL, Walker PA, Shah SK, Ewing-Cobbs L, Hasan KM, Day MC, Lee D, Jimenez F, Gee A (2011) Autologous bone marrow mononuclear cell therapy for severe traumatic brain injury in children. Neurosurgery 68: 588–600.

Dalous J, Pansiot J, Pham H, Chatel P, Nadaradja C, D'Agostino I, Vottier G, Schwendimann L, Vanneaux V, Charriaut-Marlangue C, Titomanlio L, Gressens P, Larghero J, Baud O (2012) Use of human umbilical cord blood mononuclear cells to prevent perinatal brain injury: a preclinical study. Stem Cells Dev 22:169–179.

Dammann O, Ferriero D, Gressens P (2011) Neonatal encephalopathy or hypoxic–ischemic encephalopathy? Appropriate terminology matters. Pediatr Res 70:1–2.

de Paula S, Vitola AS, Greggio S, de Paula D, Mello PB, Lubianca JM, Xavier LL, Fiori HH, Dacosta JC (2009) Hemispheric brain injury and behavioral deficits induced by severe neonatal hypoxia–ischemia in rats are not attenuated by intravenous administration of human umbilical cord blood cells. Pediatr Res 65:631–635.

de Paula S, Greggio S, Marinowic DR, Machado DC, DaCosta JC (2012) The dose-response effect of acute intravenous transplantation of human umbilical cord blood cells on brain damage and spatial memory deficits in neonatal hypoxia–ischemia. Neuroscience 210:431–441.

Donega V, van Velthoven CT, Nijboer CH, Kavelaars A, Heijnen CJ (2013) The endogenous regenerative capacity of the damaged newborn brain: boosting neurogenesis with mesenchymal stem cell treatment. J Cereb Blood Flow Metab 33:625–634.

Fujita Y, Ihara M, Ushiki T, Hirai H, Kizaka-Kondoh S, Hiraoka M, Ito H, Takahashi R (2010) Early protective effect of bone marrow mononuclear cells against ischemic white matter damage through augmentation of cerebral blood flow. Stroke 41:2938–2943.

Geißler M, Dinse HR, Neuhoff S, Kreikemeier K, Meier C (2011) Human umbilical cord blood cells restore brain damage induced changes in rat somatosensory cortex. PLoS One 6:e20194.

Hagberg H, Peebles D, Mallard C (2002) Models of white matter injury: comparison of infectious, hypoxic–ischemic, and excitotoxic insults. Ment Retard Dev Disabil Res Rev 8:30–38.

Ingram DA, Mead LE, Tanaka H, Meade V, Fenoglio A, Mortell K, Pollok K, Ferkowicz MJ, Gilley D, Yoder MC (2004) Identification of a novel hierarchy of endothelial progenitor cells using human peripheral and umbilical cord blood. Blood 104:2752–2760.

Kao CH, Chen SH, Chio CC, Lin MT (2008) Human umbilical cord blood-derived CD34$^+$ cells may attenuate spinal cord injury by stimulating vascular endothelial and neurotrophic factors. Shock 29:49–55.

Kawamoto A, Iwasaki H, Kusano K, Murayama T, Oyamada A, Silver M, Hulbert C, Gavin M, Hanley A, Ma H, Kearney M, Zak V, Asahara T, Losordo DW (2006) CD34-positive cells exhibit increased potency and safety for therapeutic neovascularization after myocardial infarction compared with total mononuclear cells. Circulation 114:2163–2169.

Kim JP, Lee YH, Lee YA, Kim YD (2007) A comparison of the kinetics of nucleated cells and CD34$^+$ cells in neonatal peripheral blood and cord blood. Biol Blood Marrow Transplant 13:478–485.

Kim ES, Ahn SY, Im GH, Sung DK, Park YR, Choi SH, Choi SJ, Chang YS, Oh W, Lee JH, Park WS (2012) Human umbilical cord blood-derived mesenchymal stem cell transplantation attenuates severe brain injury by permanent middle cerebral artery occlusion in newborn rats. Pediatr Res 72:277–284.

Lee OK, Kuo TK, Chen WM, Lee KD, Hsieh SL, Chen TH (2004) Isolation of multipotent mesenchymal stem cells from umbilical cord blood. Blood 103:1669–1675.

Majka M, Janowska-Wieczorek A, Ratajczak J, Ehrenman K, Pietrzkowski Z, Kowalska MA, Gewirtz AM, Emerson SG, Ratajczak MZ (2001) Numerous growth factors, cytokines, and chemokines are secreted by human CD34(+) cells, myeloblasts, erythroblasts, and megakaryoblasts and regulate normal hematopoiesis in an autocrine/paracrine manner. Blood 97: 3075–3085.

Meier C, Middelanis J, Wasielewski B, Neuhoff S, Roth-Haerer A, Gantert M, Dinse HR, Dermietzel R, Jensen A (2006) Spastic paresis after perinatal brain damage in rats is reduced by human cord blood mononuclear cells. Pediatr Res 59:244–249.

Murohara T, Ikeda H, Duan J, Shintani S, Sasaki K, Eguchi H, Onitsuka I, Matsui K, Imaizumi T (2000) Transplanted cord blood-derived endothelial precursor cells augment postnatal neovascularization. J Clin Invest 105:1527–1536.

Nakano-Doi A, Nakagomi T, Fujikawa M, Nakagomi N, Kubo S, Lu S, Yoshikawa H, Soma T, Taguchi A, Matsuyama T (2010) Bone marrow mononuclear cells promote proliferation of endogenous neural stem cells through vascular niches after cerebral infarction. Stem Cells 28:1292–1302.

Nelson KB, Lynch JK (2004) Stroke in newborn infants. Lancet Neurol 3:150–158.

Newcomb JD, Ajmo Jr CT, Sanberg CD, Sanberg PR, Pennypacker KR, Willing AE (2006) Timing of cord blood treatment after experimental stroke determines therapeutic efficacy. Cell Transplant 15:213–223.

Ohshima M, Tsuji M, Taguchi A, Kasahara Y, Ikeda T (2012) Cerebral blood flow during reperfusion predicts later brain damage in a mouse and a rat model of neonatal hypoxic–ischemic encephalopathy. Exp Neurol 233:481–489.

Osawa M, Hanada K, Hamada H, Nakauchi H (1996) Long-term lymphohematopoietic reconstitution by a single CD34-low/negative hematopoietic stem cell. Science 273:242–245.

Ou Y, Yu S, Kaneko Y, Tajiri N, Bae EC, Chheda SH, Stahl CE, Yang T, Fang L, Hu K, Borlongan CV, Yu G (2010) Intravenous infusion of GDNF gene-modified human umbilical cord blood CD34$^+$ cells protects against cerebral ischemic injury in spontaneously hypertensive rats. Brain Res 1366:217–225.

Palmer C, Roberts RL, Young PI (2004) Timing of neutrophil depletion influences long-term neuroprotection in neonatal rat hypoxic–ischemic brain injury. Pediatr Res 55:549–556.

Pimentel-Coelho PM, Magalhaes ES, Lopes LM, deAzevedo LC, Santiago MF, Mendez-Otero R (2010) Human cord blood transplantation in a neonatal rat model of hypoxic–ischemic brain damage: functional outcome related to neuroprotection in the striatum. Stem Cells Dev 19:351–358.

Prasad VK, Mendizabal A, Parikh SH, Szabolcs P, Driscoll TA, Page K, Lakshminarayanan S, Allison J, Wood S, Semmel D, Escolar ML, Martin PL, Carter S, Kurtzberg J (2008) Unrelated donor umbilical cord blood transplantation for inherited metabolic disorders in 159 pediatric patients from a single center: influence of cellular composition of the graft on transplantation outcomes. Blood 112:2979–2989.

Rafii S, Lyden D (2003) Therapeutic stem and progenitor cell transplantation for organ vascularization and regeneration. Nat Med 9:702–712.

Roach ES, Golomb MR, Adams R, Biller J, Daniels S, Deveber G, Ferriero D, Jones BV, Kirkham FJ, Scott RM, Smith ER, American Heart Association Stroke CCouncil on Cardiovascular Disease in the Y (2008) Management of stroke in infants and children: a scientific statement from a Special Writing Group of the American Heart Association Stroke Council and the Council on Cardiovascular Disease in the Young. Stroke 39:2644–2691.

Rosenblum S, Wang N, Smith TN, Pendharkar AV, Chua JY, Birk H, Guzman R (2012) Timing of intra-arterial neural stem cell transplantation after hypoxia–ischemia influences cell engraftment, survival, and differentiation. Stroke 43:1624–1631.

Rosenkranz K, Kumbruch S, Lebermann K, Marschner K, Jensen A, Dermietzel R, Meier C (2010) The chemokine SDF-1/CXCL12 contributes to the 'homing' of umbilical cord blood cells to a hypoxic–ischemic lesion in the rat brain. J Neurosci Res 88:1223–1233.

Rosenkranz K, Kumbruch S, Tenbusch M, Marcus K, Marschner K, Dermietzel R, Meier C (2012) Transplantation of human umbilical cord blood cells mediated beneficial effects on apoptosis, angiogenesis and neuronal survival after hypoxic–ischemic brain injury in rats. Cell Tissue Res 348:429–438.

Rosenkranz K, Tenbusch M, May C, Marcus K, Meier C (2013) Changes in Interleukin-1 alpha serum levels after transplantation of umbilical cord blood cells in a model of perinatal hypoxic–ischemic brain damage. Ann Anat 195:122–127.

Sato Y, Nakanishi K, Hayakawa M, Kakizawa H, Saito A, Kuroda Y, Ida M, Tokita Y, Aono S, Matsui F, Kojima S, Oohira A (2008) Reduction of brain injury in neonatal hypoxic–ischemic rats by intracerebroventricular injection of neural stem/progenitor cells together with chondroitinase ABC. Reprod Sci 15:613–620.

Shyu WC, Lin SZ, Chiang MF, Su CY, Li H (2006) Intracerebral peripheral blood stem cell ($CD34^+$) implantation induces neuroplasticity by enhancing beta1 integrin-mediated angiogenesis in chronic stroke rats. J Neurosci 26:3444–3453.

Sun J, Allison J, McLaughlin C, Sledge L, Waters-Pick B, Wease S, Kurtzberg J (2010) Differences in quality between privately and publicly banked umbilical cord blood units: a pilot study of autologous cord blood infusion in children with acquired neurologic disorders. Transfusion 50:1980–1987.

Taguchi A, Soma T, Tanaka H, Kanda T, Nishimura H, Yoshikawa H, Tsukamoto Y, Iso H, Fujimori Y, Stern DM, Naritomi H, Matsuyama T (2004a) Administration of $CD34^+$ cells after stroke enhances neurogenesis via angiogenesis in a mouse model. J Clin Invest 114:330–338.

Taguchi A, Matsuyama T, Moriwaki H, Hayashi T, Hayashida K, Nagatsuka K, Todo K, Mori K, Stern DM, Soma T, Naritomi H (2004b) Circulating CD34-positive cells provide an index of cerebrovascular function. Circulation 109:2972–2975.

Taguchi A, Nakagomi N, Matsuyama T, Kikuchi-Taura A, Yoshikawa H, Kasahara Y, Hirose H, Moriwaki H, Nakagomi T, Soma T, Stern DM, Naritomi H (2009) Circulating CD34-positive cells have prognostic value for neurologic function in patients with past cerebral infarction. J Cereb Blood Flow Metab 29:34–38.

Taguchi A, Kasahara Y, Nakagomi T, Stern DM, Fukunaga M, Ishikawa M, Matsuyama T (2010) A reproducible and simple model of permanent cerebral ischemia in CB-17 and SCID mice. J Exp Stroke Transl Med 3:28–33.

Tsuji M, Taguchi A, Ohshima M, Kasahara Y, Ikeda T (2012) Progesterone and allopregnanolone exacerbate hypoxic–ischemic brain injury in immature rats. Exp Neurol 233:214–220.

Tsuji M, Ohshima M, Taguchi A, Kasahara Y, Ikeda T, Matsuyama T (2013) A novel reproducible model of neonatal stroke in mice: comparison with a hypoxia–ischemia model. Exp Neurol 247:218–225.

Uemura M, Kasahara Y, Nagatsuka K, Taguchi A (2012) Cell-based therapy to promote angiogenesis in the brain following ischemic damage. Curr Vasc Pharmacol 10:285–288.

van Velthoven CT, Kavelaars A, van Bel F, Heijnen CJ (2010) Mesenchymal stem cell treatment after neonatal hypoxic–ischemic brain injury improves behavioral outcome and induces neuronal and oligodendrocyte regeneration. Brain Behav Immun 24:387–393.

van Velthoven CT, Sheldon RA, Kavelaars A, Derugin N, Vexler ZS, Willemen HL, Maas M, Heijnen CJ, Ferriero DM (2013) Mesenchymal stem cell transplantation attenuates brain injury after neonatal stroke. Stroke 44:1426–1432.

Verina T, Fatemi A, Johnston MV, Comi AM (2013) Pluripotent possibilities: human umbilical cord blood cell treatment after neonatal brain injury. Pediatr Neurol 48:346–354.

Wang XL, Zhao YS, Hu MY, Sun YQ, Chen YX, Bi XH (2013) Umbilical cord blood cells regulate endogenous neural stem cell proliferation via hedgehog signaling in hypoxic ischemic neonatal rats. Brain Res 1518:26–35.

Wasielewski B, Jensen A, Roth-Harer A, Dermietzel R, Meier C (2012) Neuroglial activation and Cx43 expression are reduced upon transplantation of human umbilical cord blood cells after perinatal hypoxic–ischemic injury. Brain Res 1487:39–53.

Xia G, Hong X, Chen X, Lan F, Zhang G, Liao L (2010) Intracerebral transplantation of mesenchymal stem cells derived from human umbilical cord blood alleviates hypoxic ischemic brain injury in rat neonates. J Perinat Med 38:215–221.

Yamagata M, Yamamoto A, Kako E, Kaneko N, Matsubara K, Sakai K, Sawamoto K, Ueda M (2013) Human dental pulp-derived stem cells protect against hypoxic–ischemic brain injury in neonatal mice. Stroke 44:551–554.

Yasuhara T, Matsukawa N, Yu G, Xu L, Mays RW, Kovach J, Deans R, Hess DC, Carroll JE, Borlongan CV (2006) Transplantation of cryopreserved human bone marrow-derived multipotent adult progenitor cells for neonatal hypoxic–ischemic injury: targeting the hippocampus. Rev Neurosci 17:215–225.

Yasuhara T, Hara K, Maki M, Xu L, Yu G, Ali MM, Masuda T, Yu SJ, Bae EK, Hayashi T, Matsukawa N, Kaneko Y, Kuzmin-Nichols N, Ellovitch S, Cruz EL, Klasko SK, Sanberg CD, Sanberg PR, Borlongan CV (2010) Mannitol facilitates neurotrophic factor up-regulation and behavioural recovery in neonatal hypoxic–ischaemic rats with human umbilical cord blood grafts. J Cell Mol Med 14:914–921.

(Accepted 6 January 2014)
(Available online 18 January 2014)

Extracellular High Mobility Group Box 1 Plays a Role in the Effect of Bone Marrow Mononuclear Cell Transplantation for Heart Failure

Masahiro Kaneko[1], Yasunori Shintani[1], Takuya Narita[1], Chiho Ikebe[1], Nobuko Tano[1], Kenichi Yamahara[2], Satsuki Fukushima[3], Steven R. Coppen[1], Ken Suzuki[1]*

1 William Harvey Research Institute, Barts and The London School of Medicine and Dentistry, Queen Mary, University of London, London, United Kingdom, **2** Department of Regenerative Medicine and Tissue Engineering, National Cerebral and Cardiovascular Center, Suita, Osaka, Japan, **3** Cardiovascular Surgery, Osaka University Graduate School of Medicine, Suita, Osaka, Japan

Abstract

Transplantation of unfractionated bone marrow mononuclear cells (BMCs) repairs and/or regenerates the damaged myocardium allegedly due to secretion from surviving BMCs (paracrine effect). However, donor cell survival after transplantation is known to be markedly poor. This discrepancy led us to hypothesize that dead donor BMCs might also contribute to the therapeutic benefits from BMC transplantation. High mobility group box 1 (HMGB1) is a nuclear protein that stabilizes nucleosomes, and also acts as a multi-functional cytokine when released from damaged cells. We thus studied the role of extracellular HMGB1 in the effect of BMC transplantation for heart failure. Four weeks after coronary artery ligation in female rats, syngeneic male BMCs (or PBS only as control) were intramyocardially injected with/without anti-HMGB1 antibody or control IgG. One hour after injection, ELISA showed that circulating extracellular HMGB1 levels were elevated after BMC transplantation compared to the PBS injection. Quantitative donor cell survival assessed by PCR for male-specific *sry* gene at days 3 and 28 was similarly poor. Echocardiography and catheterization showed enhanced cardiac function after BMC transplantation compared to PBS injection at day 28, while this effect was abolished by antibody-neutralization of HMGB1. BMC transplantation reduced post-infarction fibrosis, improved neovascularization, and increased proliferation, while all these effects in repairing the failing myocardium were eliminated by HMGB1-inhibition. Furthermore, BMC transplantation drove the macrophage polarization towards alternatively-activated, anti-inflammatory M2 macrophages in the heart at day 3, while this was abolished by HMGB1-inhibition. Quantitative RT-PCR showed that BMC transplantation upregulated expression of an anti-inflammatory cytokine *IL-10* in the heart at day 3 compared to PBS injection. In contrast, neutralizing HMGB1 by antibody-treatment suppressed this anti-inflammatory expression. These data suggest that extracellular HMGB1 contributes to the effect of BMC transplantation to recover the damaged myocardium by favorably modulating innate immunity in heart failure.

Citation: Kaneko M, Shintani Y, Narita T, Ikebe C, Tano N, et al. (2013) Extracellular High Mobility Group Box 1 Plays a Role in the Effect of Bone Marrow Mononuclear Cell Transplantation for Heart Failure. PLoS ONE 8(10): e76908. doi:10.1371/journal.pone.0076908

Editor: Maria Cristina Vinci, Cardiological Center, Italy

Received June 5, 2013; **Accepted** August 27, 2013; **Published** October 18, 2013

Funding: This work was funded by the Barts and The London Charity Large Project Grant (422/433) and supported by NIHR-funded Barts Cardiovascular Biomedical Research Unit. This study was also funded by the Medical Research Council, UK (Senior Fellowship G116/158 to KS). The funders had no role in study design, data collection and analysis, decision to publish, or preparation of the manuscript.

Competing Interests: The authors have declared that no competing interests exist.

* E-mail: ken.suzuki@qmul.ac.uk

Introduction

Transplantation of stem or progenitor cells is an emerging approach to repair and/or regenerate damaged myocardium undergoing adverse ventricular remodeling. Unfractionated bone marrow mononuclear cells (BMCs) contain several kinds of stem/progenitor cells and are the most frequently used donor cell type in clinical cell therapy to the heart [1]. The therapeutic effect of BMC transplantation in not only acute myocardial infarction (MI) but also post-MI chronic heart failure (ischemic cardiomyopathy) has been confirmed in animal and human studies [1–3]. Because injected BMCs do not vigorously differentiate to functioning cardiomyocytes or vascular cells *in vivo*, the major mechanism of the therapeutic effects is proposed to be their secretion of cytokines, chemokines and growth factors that help repair of the damaged myocardium suffering post-MI adverse remodeling [1–3]. However, the precise mechanism of this "paracrine effect" remains uncertain.

Interestingly, cardiac function recovery by BMC transplantation occurs despite of markedly poor donor cell survival [1,3,4]. It has also been shown that active secretion from BMCs is less extensive compared to other donor cell types [5,6]. It was also reported that injection of extract of dead BMCs by freeze-thaw cycles induces the similar therapeutic effect to injection of living BMCs [7]. These findings led us to hypothesize that dead donor BMCs might be a supplementary or alternative source of the paracrine mediators, which could contribute to the repair of the failing myocardium.

High-mobility group box 1 (HMGB1) was initially identified as a nuclear protein that regulates transcriptional factors to stabilize the nucleosome [8]. This molecule is also known to be actively secreted from activated inflammatory cells and also passively

released from dead cells [9–11]. Extracellular HMGB1 induces and intensifies inflammation in most cases, while it can also operate to attenuate inflammation and enhance the healing of damaged tissues, according to the form/amount of HMGB1 and nature of the tissues [9–12]. In the heart, there is increasing evidence that extracellular HMGB1 attenuates myocardial damage and induces recovery/regeneration [13–18], though there are contradicting reports [19,20]. We have demonstrated that HMGB1 administration achieved the similar benefits to the BMC-mediated paracrine effects, including decreased fibrosis, increased vascular formation, attenuated cardiomyocyte hypertrophy, and attenuated inflammation in a rat ischemic cardiomyopathy model [17]. It has also been reported that extracellular HMGB1 augments tissue regeneration through activating endogenous progenitor cells [15,21].

Collectively, these data formed a hypothesis that extracellular HMGB1 released from dead donor cells contributes to the paracrine effect of BMC transplantation to repair the post-MI failing myocardium and to improve cardiac performance.

Materials and Methods

Ethics Statement

All studies were performed with the approval of the UK Home Office (Project Licence Number: 70/7254). The investigation conforms to the Principles of Laboratory Animal Care formulated by the National Society for Medical Research and the Guide for the Care and Use of Laboratory Animals (US NIH Publication, 1996). All animal surgery was performed under inhalation anesthesia of isoflurane and administration of buprenorphine hydrochloride was made just after surgery to reduce postoperative pain, and all efforts were made to minimize suffering. Surgical procedures, cardiac function measurement, and sample analyses were performed in a blinded manner.

BMC Collection

Bone marrow was isolated from both femurs and tibias of male Lewis rats (150–200 g; Charles River, UK), from which BMCs (mononuclear cells) were purified by Ficoll-Paque gradient centrifugation (GE Healthcare) as previously described [3]. Flow cytometry analysis (FACSAria, BD Biosciences) using monoclonal anti-rat CD34 (Santa-Cruz) and anti-rat CD45 (BD Pharmingen) antibodies showed that 4.6±1.7% of the BMCs were positive for CD34 and 75.5±4.3% were positive for CD45 (**Figure S1**). To trace the injected cells, BMCs were labeled with CM-DiI (Molecular Probes) before transplantation according to the company's protocol. The viability of donor BMCs just before injection measured by trypan blue staining was 97.1±0.6% (n = 11 animals).

Assessment of Cardiac Function

Cardiac function and dimensions pre and post treatment were measured by using echocardiography (Vevo−770, VisualSonics) as previously described [3,17]. Diastolic and systolic LV endocardial areas at the papillary muscle level were measured from parasternal short-axis views, from which LV fractional area change (LVFAC) was calculated. Post treatment hemodynamics parameters were measured by catheterization (SRP−320/PVAN3.2, Millar Instruments and Chart 5 software, ADInstruments) as described previously [22].

Generation of Ischemic Cardiomyopathy and Cell Transplantation in Rat

Female Lewis rats (150–200 g, Charles River) underwent left coronary artery ligation as described previously [3,17,23,24]. Four weeks later, the animals that showed appropriate cardiac dysfunction (LVFAC 22–32%; base line in intact rats = 61.6±1.7% [n = 5]) by echocardiography were chosen and randomly assigned to 4 treatment groups; intramyocardial injection of 1×10^7 syngeneic male BMCs (BMC group), injection of BMCs with 50 μg anti-HMGB1 neutralizing antibody (Medical & Biological Laboratories; AB group), injection of BMCs with 50 μg control IgG (Sigma-Aldrich; IgG group), and injection of PBS only (CON group). BMCs were suspended in 200 μl of PBS and intramyocardial injection was performed into 2 sites (100 μl each) of the LV free wall, targeting the border areas [3].

To optimize the antibody dose, 1×10^7 BMCs were injected with 0, 10, 50, or 100 μg of anti-HMGB1 antibody in the same model (n≥3). At day 28, LVFAC was 31.5±1.2, 30.3±1.5, 26.6±1.3, and 26.4±1.8%, respectively. Then, 50 μg antibody was used in the main study.

Detection of Released HMGB1

Peripheral blood was collected, from which serum was obtained by centrifugation. HMGB1 levels in the serum were determined in duplicate using a commercial ELISA kit (IBL international GMBH) according to the manufacture's instruction.

Histological Analysis

The hearts were excised, fixed with 4% paraformaldehyde, embedded in OCT compound, and quickly frozen in liquid nitrogen. Cryosections were cut and incubated with biotin conjugated Griffonia simplicifolia lectin I-isolectin B4 (1:100, Vector), monoclonal anti-rat CD68 antibody (1:100, AbD Serotec), monoclonal anti-rat CD86 antibody (1:50, BD), monoclonal anti-rat CD163 antibody (1:100, AbD Serotec), monoclonal anti-rat Ki-67 antibody (1:50, DakoCytomation), and/or polyclonal anti-rat cardiac troponin-T (cTnT) antibody (1:200, HyTest) followed by visualization using appropriate fluorophore-conjugated secondary antibodies (Molecular Probes). Samples were observed by a fluorescence microscopy (BZ8000, Keyence) with or without nuclear counter-staining using 4′, 6-diamidino-2-phenylindole (DAPI). Ten different fields were randomly selected in each border area of the samples and assessed. Another set of sections were stained with 0.1% picrosirius red, which enabled calculation of extracellular collagen volume fraction in border area by using NIH image-analysis software [3,17,22].

Quantitative Analysis of Donor Cell Survival

Genomic DNA was extracted from the whole LV samples of female rats. To detect donor cell (male) survival, expression of the Y chromosome-specific *sry* gene in these samples was assessed by real-time polymerase chain reaction (PCR; Prism 7900HT, Applied Biosystems). The *sry* levels were normalized to the DNA amount using the autosomal single copy gene, oesteopontin. The number of surviving donor cells was estimated by correcting the relative *sry* expression using a standard curve as previously described [3,17,22].

Measurements of Myocardial Gene Expression

Total RNA was extracted from the whole LV samples and assessed for myocardial expression of *IL-1β*, *TNF-α*, and *IL-10* by quantitative RT-PCR (Prism 7900HT, Applied Biosystems) as previously described [22]. TaqMan primers and probes were

purchased from Applied Biosystems. Expression was normalized using *Ubiquitin C*.

Statistical Analysis

All values are expressed as mean±SEM. Statistical comparison of the data was performed using the student's unpaired *t*-test for the analysis of circulating HMGB1 levels. All other data were analyzed with one-way ANOVA followed by Fisher's post-hoc analysis to compare groups. A value of $p<0.05$ was considered statistically significant.

Results

Poor Donor Cell Survival and Increased Extracellular HMGB1 After BMC Transplantation

Female rats suffering ischemic cardiomyopathy were randomly assigned to 4 groups; intramyocardial injection of syngeneic male BMCs (BMC group), intramyocardial injection of male BMCs with anti-HMGB1 neutralizing antibody (AB group), intramyocardial injection of male BMCs with control IgG (IgG group), and intramyocardial injection of PBS only (CON group). After each treatment, quantitative PCR for the male-specific *sry* gene demonstrated that donor cell survival after BMC transplantation was poor similarly in the BMC, AB, and IgG groups; below 10% at day 3, further decreasing to below 1% by day 28 (**Figure 1A**). Histological analysis detected islet-like clusters of donor cells at day 3 after BMC transplantation (**Figure 1B**). ELISA showed that the circulating extracellular HMGB1 level was 2.5-fold elevated one hour after BMC transplantation, compared to the PBS injection control (**Figure 1C**).

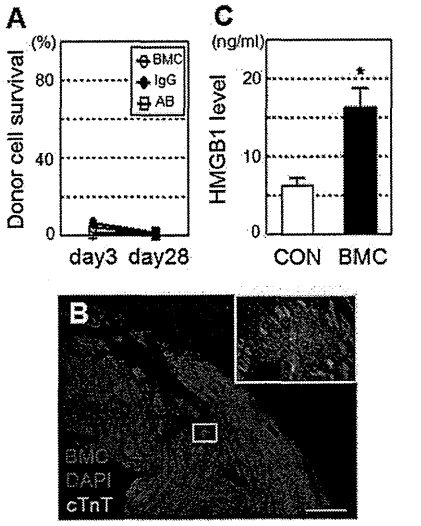

Figure 1. Poor donor cell survival and HMGB1 leakage after BMC transplantation. (**A**) Quantitative PCR for the male specific *sry* gene showed that the survival of male donor cells in female hearts was poor similarly in the BMC (BMC injection), IgG (BMC+control IgG injection), and AB (BMC+anti-HMGB1 antibody injection) groups at both days 3 and 28; n=5~7 in each point. (**B**) Clusters of DiI-labeled (red) donor BMCs were detected in the heart at day 3 after BMC transplantation. A higher magnification image of the yellow frame is shown. Green=cardiomyocytes (cTnT); blue=nuclei (DAPI). Scale bar=300 μm. (**C**) ELISA showed that the circulating HMGB1 level was increased at 1 hour in the BMC group compared to the PBS injection control (CON group). *:$p<0.05$ *versus* the CON group, mean±SEM for n=5 each.
doi:10.1371/journal.pone.0076908.g001

Abolished BMC Transplantation-induced Cardiac Function Recovery by HMGB1-inhibition

Four weeks after BMC transplantation (BMC group), echocardiography and cardiac catheterization consistently demonstrated that both systolic and diastolic LV function, in terms of LV fractional area change, max and min dP/dt, and systolic pressure, was improved compared to the control (CON group; **Figure 2**). Enlargement of LV systolic endocardial area in the control group was attenuated by BMC transplantation. Of note, these effects were largely abolished by HMGB1-inhibition (AB group), but not by control IgG administration (IgG group), indicating an important role of extracellular HMGB1 in the therapeutic benefits of BMC transplantation.

Elimination of BMC Transplantation-induced Tissue Recovery by HMGB1-inhibition

To investigate the mechanism by which extracellular HMGB1 released in BMC transplantation improved post-MI cardiac function, we performed a set of histological studies with a focus on the paracrine effect. Consistent to previous reports [3], BMC transplantation (BMC group) attenuated post-MI pathological fibrosis, improved neovascular formation, and increased proliferation activity in the border areas at day 28, compared to the control (CON group; **Figure 3 and Figure S2**). All these paracrine effects were, however, eliminated by HMGB1-inhibition (AB group), but not by IgG administration (IgG group), corresponding to the cardiac function change as shown in Figure 2.

Modulation of M2/M1 Macrophage Polarization by BMC Transplantation through HMGB1

Additional immunolabeling showed that BMC transplantation increased myocardial accumulation of $CD68^+$ pan-macrophages compared to the control (**Figure 4A and Figure S3A, B**). Here, the increase in $CD86^+$ classically-activated pro-inflammatory (M1) macrophages was trivial (**Figure 4B and Figure S3D, E**), while the enhancement of $CD163^+$ alternatively-activated (M2) macrophages was more obvious (**Figure 4C and Figure S3G, H**). As a result, the ratio of M2/M1 macrophage in the BMC group (92.9/36.9=2.52) was increased from 56.3/28.4=1.98 in the CON group. Of note, HMGB1-inhibition abolished the enhancement of $CD163^+$ M2 macrophages (**Figure 4C and Figure S3I**) and exacerbated the increase in $CD86^+$ M1 macrophages (**Figure 4B and Figure S3F**), thus largely reducing the M2/M1 ratio to 67.6/62.9=1.07. These results suggest that the HMGB1-mediated shift of macrophage polarization towards anti-inflammatory M2 macrophages might play a role in the BMC transplantation-induced myocardial recovery.

Quantitative RT-PCR showed that myocardial expression of the anti-inflammatory cytokine, *IL-10*, tended to be elevated by BMC transplantation compared to the control, while this was totally eliminated by inhibiting HMGB1 (**Figure 4D**). IL-10 is known to be secreted by alternatively activated M2 macrophages and also by Th2 cells that induce M2 macrophage differentiation [9,25,26]. The expression of *IL-1β* or *TNF-α* was not affected by either BMC transplantation or HMGB1-inhibition (**Figure 4E, F**).

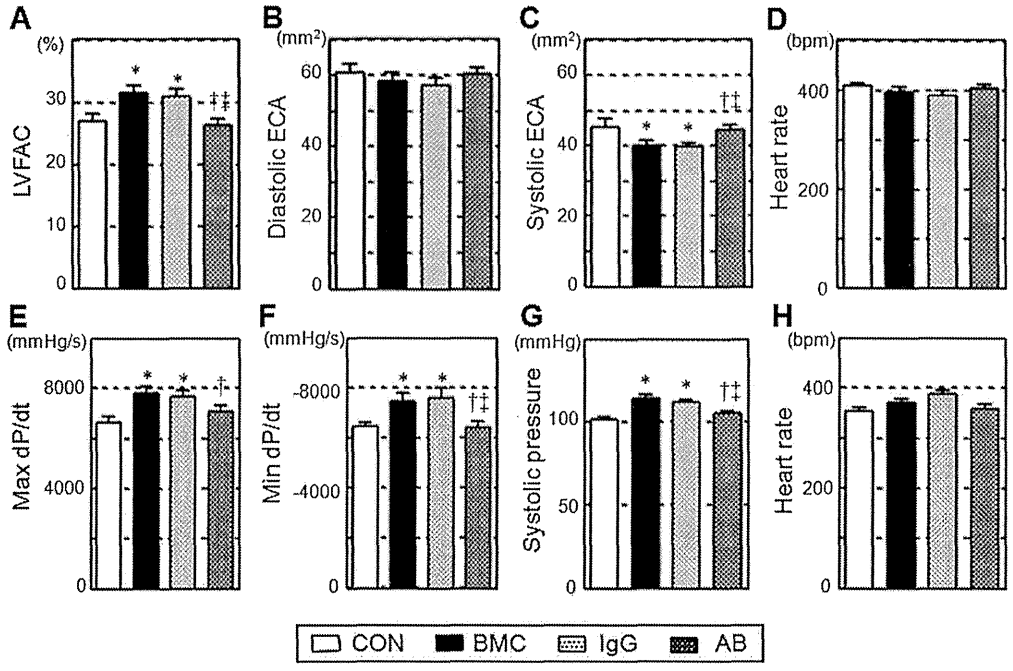

Figure 2. Abolished BMC transplantation-induced cardiac function recovery by HMGB1-inhibition. Cardiac parameters were measured by echocardiography (**A–D**) and catheterization (**E–H**) on day 28 after each treatment. Cardiac function was improved by BMC transplantation (BMC group) compared to the PBS injection control (CON group), while this effect was eliminated by antibody neutralization of HMGB1 (AB group), but not by control IgG administration (IgG group). LVFAC, left ventricular fractional area change; ECA, endocardial area. *:$p<0.05$ *versus* the CON group, †:$p<0.05$ *versus* the BMC group. ‡:$p<0.05$ *versus* the IgG group, mean±SEM for n=8~10 in each group.
doi:10.1371/journal.pone.0076908.g002

Discussion

Using a post-MI ischemic cardiomyopathy model in rat, we demonstrated that the BMC transplantation-mediated benefits, including increased neovascular formation, reduced collagen deposition, increased proliferation activity, favorable modulation of macrophage polarization, and resultant improvement of cardiac function, were all eliminated by antibody-neutralization of HMGB1. These data suggest that extracellular HMGB1 plays a role in the effects of BMC transplantation to recover the failing myocardium undergoing post-MI adverse remodeling and to improve global cardiac function. This finding is validated by the consistency with the previous report demonstrating that administration of recombinant HMGB1 protein achieved the same benefits as the BMC transplantation-mediated effects using the similar ischemic heart failure model in rats [17].

In view of the origin of extracellular HMGB1 occurring after BMC transplantation into post MI chronic heart failure, there are 4 theoretically possible sources: (i) passive release from dead donor BMCs, (ii) passive release from dead host (endogenous) cells, (iii) active secretion from surviving donor BMCs, and (iv) active secretion from host (endogenous) cells. It is likely that the major origin may be (i) passive release from dead donor BMCs, given the following information. [I] Survival of donor BMCs was largely limited, indicating that there was a considerable amount of donor cell death; [II] In this model of ischemic cardiomyopathy, death/damage of host cells in the heart and other organs by BMC injection is unlikely to be substantial; [III] There was an increased level of circulating HMGB1 as early as 1 hour after BMC injection. This time course is too rapid for inflammatory cells to actively secrete HMGB1 *via* transcription after stimulation [9,27]. Having said these, we could not eliminate the possibility that extracellular HMGB1 from other sources, particularly from endogenous sources (host cells), might contribute to the paracrine effect of BMC transplantation. Experiments using HMGB1-deficient BMCs, either by knockout or knockdown, as donor would provide useful information to this point. However, HMGB1 knockout mice die immediately after birth [28], while on the other hand reproducible and satisfactory knockdown in primary rat unfractionated BMCs has not been established.

The role of extracellular HMGB1 to attenuate myocardial damage and to induce recovery and/or regeneration remains controversial [13–20]. This discrepancy may be relevant to different types of HMGB1 and different conditions of the host myocardium. In the settings of acute MI (without cell transplantation), a large amount of HMGB1 is actively secreted from accumulated inflammatory cells in addition to HMGB1 passively released from a large number of dead host cardiac cells. The dynamics and functions of these different types of HMGB1 are likely to be distinct, due to different phosphorylation, acetylation, and formation of complexes by binding other pathogenic molecules [9,11]. Delicate balance between these types of extracellular HMGB1 may affect the overall effect, whether beneficial or harmful, of HMGB1. Our study therefore used a post-MI ischemic cardiomyopathy model to exclude these contaminating factors. The degree of HMGB1 both from inflammatory cells and dead host cardiac cells in this model is presumed to be much less than that in acute MI settings, and the frequency of host cardiac cell death by BMC injection is also negligible, compared to donor cell death.

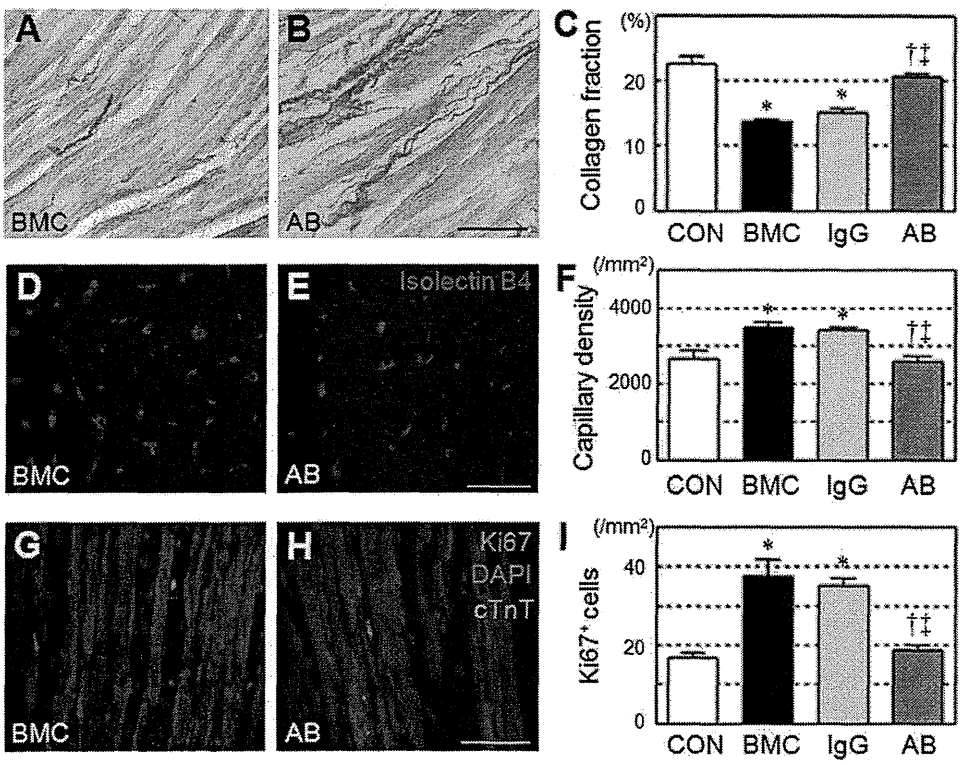

Figure 3. Eliminated BMC transplantation-induced tissue recovery by HMGB1-inhibition. Reduced extracellular collagen deposition (**A–C;** picrosirius red = red), increased capillary density (**D–F;** Isolectin B4 = red), and increased proliferation (**G–I;** Ki67 = red; nuclei = blue; cTnT = green) were observed in the border areas at day 28 after BMC transplantation (BMC group), compared to the PBS control (CON group). These effects were all abolished by anti-HMGB1 antibody neutralization (AB group), but not by control IgG administration (IgG group). Representative images of only BMC and AB groups are present (see **Figure S2** for additional images). Scale bars = 50 μm in **A, B, G, H** and 30 μm in **D, E.** *:$p<0.05$ *versus* the CON group, †:$p<0.05$ *versus* the BMC group, ‡:$p<0.05$ *versus* the IgG group, mean±SEM for n = 5~7 in each group.
doi:10.1371/journal.pone.0076908.g003

It will be interesting to investigate whether the present results in unfractionated BMCs are applicable to other types of donor cells. There are published data in other cell types that appear to be contradicting to our findings in BMCs at a glance. Ziebart *et al.* have reported that the persistence of donor cells contributes to the therapeutic effect of transplantation of endothelial progenitor cells

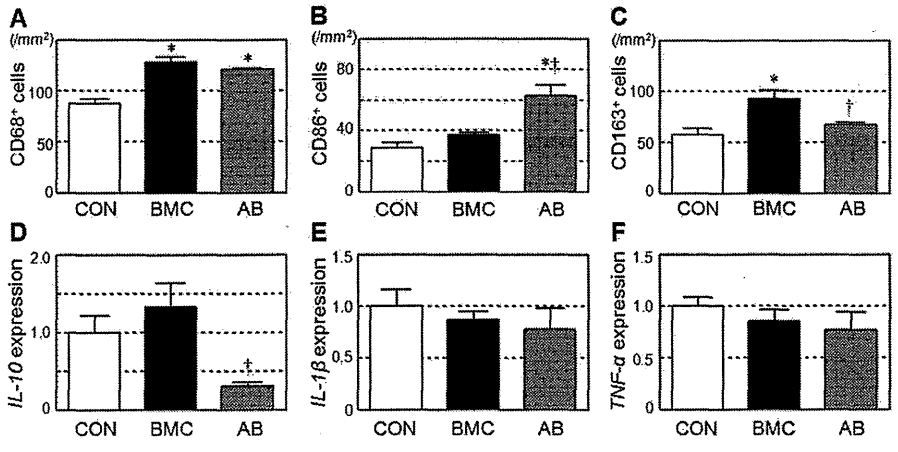

Figure 4. Modulation of innate immunity by BMC transplantation via released HMGB1. Accumulation of $CD68^+$ pan-macrophages (**A**), $CD86^+$ classically-activated pro-inflammatory M1 macrophages (**B**), and $CD163^+$ alternatively-activated anti-inflammatory M2 macrophages (**C**) in the border areas at day 3 after each treatment was assessed by immunolabeling. See **Figure S3** for representative images. Myocardial expression of *IL-10* (**D**), *IL-1β* (**E**)), and *TNF-α* (**F**) at day 3 after each treatment was measured by quantitative RT-PCR. *:$p<0.05$ *versus* the CON group, †:$p<0.05$ *versus* the BMC group, mean±SEM for n = 5~7 in each group.
doi:10.1371/journal.pone.0076908.g004

by using the inducible suicide gene [29]. Laflamme *et al.* have demonstrated that increase of donor cell presence (thus reducing donor cell death) by the treatment with pro-survival factors enhances therapeutic effects of transplantation of embryonic stem cell-derived cardiomyocytes [30]. However, in contrast, in the case of unfractionated BMCs, Yeghiazarians *et al.* reported that ultrasound-guided injection of extract of dead BMCs by freeze-thaw cycles achieves the similar therapeutic effect to injection of living BMCs [7], supporting our findings. This cell type-dependent controversy may suggest that the impact of HMGB1 released from dead donor cells to recover the damaged myocardium could be diluted/hidden in the case of transplantation of "more proficient" cells such as endothelial progenitor cells and embryonic stem cell-derived cardiomyocytes that have more substantial abilities of beneficial differentiation, secretion, and/or contraction. In addition, the extent and/or types of donor cell death after transplantation may vary according to donor cell types, affecting the release of HMGB1. Differences in the condition of the host heart, *i.e.* acute MI *versus* post-MI ischemic cardiomyopathy, may also influence the impact of extracellular HMGB1 from donor cells. Further studies to elucidate the role of extracellular HMGB1 in different donor cell types in the same experimental setting are warranted.

Macrophages are an important player in the progress and recovery of post-MI adverse ventricular remodeling [31,32]. It has also been shown that HMGB1 and receptor for advanced glycation endproducts signaling play a role in the macrophage-involved tissue repair mechanism in the peripheral nerve [33]. Recent research has shown that macrophages can be functionally polarized into classically-activated M1 (pro-inflammatory) or alternatively-activated M2 (anti-inflammation and tissue healing) phenotypes according to the environmental condition [9,26]. Stimulation with IFN-γ or TNF-α drives the macrophages into the M1 phenotype, which is characterized by a strong pro-inflammatory ability. In contrast, exposure to IL-4 or IL-13 generates M2 macrophages, which attenuate inflammation and enhance tissue recovery and healing. Importance of this polarization balance in the repair of damaged organs, including the heart, has been reported [9,26]. Our results here uncovered that BMC transplantation enhanced "beneficial" M2 macrophages in the heart, for which extracellular HMGB1 was responsible. Therefore, HMGB1-mediated modulation of the macrophage's polarization towards the M2 phenotype might be a part of the mechanism by which BMC transplantation recovers the damaged myocardium and improves cardiac function. Further study should focus on elucidation of the molecular mechanism of extracellular HMGB1 to modulate the M1/M2 macrophage polarization, in a simpler model.

A limitation of this study may be that our conclusion is based on the antibody neutralization experiments, which might carry a risk (though unlikely) of unexpected artifacts, such as unpredictable actions of the immune complexes generated. Investigations using HMGB1-deficient cells, either by knockout or knockdown, could add useful validation of our results, but these were not practical due to technical limitations as discussed above. Nonetheless, the consistency with the previous evidence that administration of HMGB1 protein induces the same effects as the BMC transplantation [17] supports our results.

In summary, our results demonstrated that extracellular HMGB1, which is derived from dead donor cells at least in part, plays a role of the effect of BMC transplantation to recover the damaged tissue by favorably modulating innate immunity in heart failure. This novel proof-of-concept will imply an important clue to further understand and refine BMC transplantation therapy for heart failure.

Supporting Information

Figure S1 Characterisation of BMCs by flow cytometry analysis. Flow cytometry analysis showed that 4.6±1.7%of collected rat BMCs were positive for CD34 and 75.5±4.3% were positive for CD45. A representative image is presented.
(TIF)

Figure S2 Supplement to Figure 3; HMGB1-inhibition abolished myocardial recovery by BMC transplantation. **A–D:** Representative images of picrosirius red staining. Scale bar = 50 μm. **E–H:** Representative images of islectin-B4 staining (red). Scale bar = 30 μm. **I–L:** Representative images of immunofluorescent labelling with Ki-67 (red); blue = nuclei (DAPI). Scale bar = 50 μm.
(TIF)

Figure S3 Supplement to Figure 4; Inflammation was modulated by BMC transplantation through HMGB1. Representative images of immunofluorescent labelling with CD68 (**A–C**), CD86 (**D–F**), and CD163 (**G–I**). Green is for each target molecule; blue for nuclei (DAPI). Scale bars = 50 μm.
(TIF)

Acknowledgments

We thank Drs Niall Campbell and Kenta Yashiro (Ken Suzuki laboratory) for their technical assistance and scientific suggestions.

Author Contributions

Conceived and designed the experiments: KS MK SRC. Performed the experiments: MK YS TN NT CI KY SF. Analyzed the data: KS MK SRC. Wrote the paper: KS MK SRC.

References

1. van Ramshorst J, Rodrigo SF, Schalij MJ, Beeres SL, Bax JJ, et al. (2011) Bone marrow cell injection for chronic myocardial ischemia: the past and the future. J Cardiovasc Transl Res 4: 182–191. doi: 10.1007/s12265-010-9249-8.
2. Donndorf P, Kundt G, Kaminski A, Yerebakan C, Liebold A, et al. (2011) Intramyocardial bone marrow stem cell transplantation during coronary artery bypass surgery: a meta-analysis. J Thorac Cardiovasc Surg 142: 911–920. doi: 10.1016/j.jtcvs.2010.12.013.
3. Fukushima S, Varela-Carver A, Coppen SR, Yamahara K, Felkin LE, et al. (2007) Direct intramyocardial but not intracoronary injection of bone marrow cells induces ventricular arrhythmias in a rat chronic ischemic heart failure model. Circulation 115: 2254–2261. doi: 10.1161/CIRCULATIONAHA.106.662577.
4. George JC, Goldberg J, Joseph M, Abdulhameed N, Crist J, et al. (2008) Transvenous intramyocardial cellular delivery increases retention in comparison to intracoronary delivery in a porcine model of acute myocardial infarction. J Interv Cardiol 21: 424–431. doi: 10.1111/j.1540-8183.2008.00390.x.
5. Ohnishi S, Yasuda T, Kitamura S, Nagaya N (2007) Effect of hypoxia on gene expression of bone marrow-derived mesenchymal stem cells and mononuclear cells. Stem Cells 25: 1166–1177. doi: 10.1634/stemcells.2006-0347.
6. Sekiguchi H, Ii M, Losordo DW (2009) The relative potency and safety of endothelial progenitor cells and unselected mononuclear cells for recovery from myocardial infarction and ischemia. J Cell Physiol 219: 235–242. doi: 10.1002/jcp.21672.
7. Yeghiazarians Y, Zhang Y, Prasad M, Shih H, Saini SA, et al. (2009) Injection of bone marrow cell extract into infarcted hearts results in functional improvement comparable to intact cell therapy. Mol Ther 17: 1250–1256. doi: 10.1038/mt.2009.85.
8. Stros M (2010) HMGB proteins: interactions with DNA and chromatin. Biochim Biophys Acta 1799: 101–113. doi: 10.1016/j.bbagrm.2009.09.008.

9. Andersson U, Tracey KJ (2011) HMGB1 is a therapeutic target for sterile inflammation and infection. Annu Rev Immunol 29: 139–162. doi: 10.1146/annurev-immunol-030409-101323.
10. Scaffidi P, Misteli T, Bianchi ME (2002) Release of chromatin protein HMGB1 by necrotic cells triggers inflammation. Nature 418: 191–195. doi: 10.1038/nature00858.
11. Yanai H, Ban T, Taniguchi T (2012) High-mobility group box family of proteins: ligand and sensor for innate immunity. Trends Immunol 33: 633–640. doi: 10.1016/j.it.2012.10.005.
12. Popovic PJ, DeMarco R, Lotze MT, Winikoff SE, Bartlett DL, et al. (2006) High mobility group B1 protein suppresses the human plasmacytoid dendritic cell response to TLR9 agonists. J Immunol 177: 8701–8707.
13. Kitahara T, Takeishi Y, Harada M, Niizeki T, Suzuki S, et al. (2008) High-mobility group box 1 restores cardiac function after myocardial infarction in transgenic mice. Cardiovasc Res 80: 40–46. doi: 10.1093/cvr/cvn163.
14. Limana F, Esposito G, D'Arcangelo D, Di Carlo A, Romani S, et al. (2011) HMGB1 attenuates cardiac remodelling in the failing heart via enhanced cardiac regeneration and miR-206-mediated inhibition of TIMP-3. PLoS One 6: e19845. doi: 10.1371/journal.pone.0019845.
15. Limana F, Germani A, Zacheo A, Kajstura J, Di Carlo A, et al. (2005) Exogenous high-mobility group box 1 protein induces myocardial regeneration after infarction via enhanced cardiac C-kit+ cell proliferation and differentiation. Circ Res 97: e73–83. doi: 10.1161/01.RES.0000186276.06104.
16. Oozawa S, Mori S, Kanke T, Takahashi H, Liu K, et al. (2008) Effects of HMGB1 on ischemia-reperfusion injury in the rat heart. Circ J 72: 1178–1184. doi: 10.1253/circj.72.1178.
17. Takahashi K, Fukushima S, Yamahara K, Yashiro K, Shintani Y, et al. (2008) Modulated inflammation by injection of high-mobility group box 1 recovers post-infarction chronically failing heart. Circulation 118: S106–114. doi: 10.1161/CIRCULATIONAHA.107.757443.
18. Zhou X, Hu X, Xie J, Xu C, Xu W, et al. (2012) Exogenous high-mobility group box 1 protein injection improves cardiac function after myocardial infarction: involvement of Wnt signaling activation. J Biomed Biotechnol 2012: 743879. doi: 10.1155/2012/743879.
19. Andrassy M, Volz HC, Igwe JC, Funke B, Eichberger SN, et al. (2008) High-mobility group box-1 in ischemia-reperfusion injury of the heart. Circulation 117: 3216–3226. doi: 10.1161/CIRCULATIONAHA.108.769331.
20. Xu H, Yao Y, Su Z, Yang Y, Kao R, et al. (2011) Endogenous HMGB1 contributes to ischemia-reperfusion-induced myocardial apoptosis by potentiating the effect of TNF-α/JNK. Am J Physiol Heart Circ Physiol 300: H913–921. doi: 10.1152/ajpheart.00703.2010.
21. Chavakis E, Hain A, Vinci M, Carmona G, Bianchi ME, et al. (2007) High-mobility group box 1 activates integrin-dependent homing of endothelial progenitor cells. Circ Res 100: 204–212. doi: 10.1161/01.RES.0000257774.55970.f4.
22. Narita T, Shintani Y, Ikebe C, Kaneko M, Harada N, et al. (2013) The use of cell-sheet technique eliminates arrhythmogenicity of skeletal myoblast-based therapy to the heart with enhanced therapeutic effects. Int J Cardiol 168: 261–269. doi: 10.1016/j.ijcard.2012.09.081.
23. Omura T, Yoshiyama M, Takeuchi K, Hanatani A, Kim S, et al. (2000) Differences in time course of myocardial mRNA expression in non-infarcted myocardium after myocardial infarction. Basic Res Cardiol 95: 316–323. doi: 10.1007/s003950070051.
24. Francic J, Weiss RM, Wei SG, Johnson AK, Felder RB (2001) Progression of heart failure after myocardial infarction in the rat. Am J Physiol Regul Integr Comp Physiol 281: R1734–1745.
25. Ouyang W, Rutz S, Crellin NK, Valdez PA, Hymowitz SG (2011) Regulation and functions of the IL-10 family of cytokines in inflammation and disease. Annu Rev Immunol 29: 71–109. doi: 10.1146/annurev-immunol-031210-101312.
26. Sica A, Mantovani A (2012) Macrophage plasticity and polarization: in vivo veritas. J Clin Invest 122: 787–795. doi: 10.1172/JCI59643.
27. Tang D, Shi Y, Jang L, Wang K, Xiao W, et al. (2005) Heat shock response inhibits release of high mobility group box 1 protein induced by endotoxin in murine macrophages. Shock 23: 434–440.
28. Calogero S, Grassi F, Aguzzi A, Voigtlander T, Ferrier P, et al. (1999) The lack of chromosomal protein Hmg1 does not disrupt cell growth but causes lethal hypoglycaemia in newborn mice. Nat Genet 22: 276–280. doi: 10.1038/10338.
29. Ziebart T, Yoon CH, Trepels T, Wietelmann A, Braun T, et al. (2008) Sustained persistence of transplanted proangiogenic cells contributes to neovascularization and cardiac function after ischemia. Circ Res 103: 1327–1334. doi: 10.1161/CIRCRESAHA.108.180463.
30. Laflamme MA, Chen KY, Naumova AV, Muskheli V, Fugate JA, et al. (2007) Cardiomyocytes derived from human embryonic stem cells in pro-survival factors enhance function of infarcted rat hearts. Nat Biotechnol 25: 1015–1024. doi: 10.1038/nbt1327.
31. Frangogiannis NG (2012) Regulation of the inflammatory response in cardiac repair. Circ Res 110: 159–173. doi: 10.1161/CIRCRESAHA.111.243162.
32. Hu Y, Zhang H, Lu Y, Bai H, Xu Y, et al. (2011) Class A scavenger receptor attenuates myocardial infarction-induced cardiomyocyte necrosis through suppressing M1 macrophage subset polarization. Basic Res Cardiol 106: 1311–1328. doi: 10.1007/s00395-011-0204-x.
33. Rong LL, Yan SF, Wendt T, Hans D, Pachydaki S, et al. (2004) RAGE modulates peripheral nerve regeneration via recruitment of both inflammatory and axonal outgrowth pathways. FASEB J 18: 1818–1825. doi: 10.1096/fj.04-1900com.

Neuroscience Research 76 (2013) 163–168

Contents lists available at SciVerse ScienceDirect

Neuroscience Research

journal homepage: www.elsevier.com/locate/neures

A highly reproducible model of cerebral ischemia/reperfusion with extended survival in CB-17 mice

Yukiko Kasahara[a], Masafumi Ihara[a], Takayuki Nakagomi[b], Yoshihiro Momota[c], David M. Stern[d], Tomohiro Matsuyama[b], Akihiko Taguchi[a,*]

[a] Department of Regenerative Medicine Research, Institute of Biomedical Research and Innovation, Hyogo, Japan
[b] Institute for Advanced Medical Sciences, Hyogo College of Medicine, Hyogo, Japan
[c] Department of Anesthesiology, Osaka Dental University, Osaka, Japan
[d] Executive Dean's Office, University of Tennessee, TN, USA

ARTICLE INFO

Article history:
Received 16 October 2012
Received in revised form 13 March 2013
Accepted 3 April 2013
Available online 18 April 2013

Keywords:
Stroke model
Transient cerebral ischemia
Ischemia/reperfusion injury
Reproducibility

ABSTRACT

To simulate the clinical and pathologic situation in patients with stroke, as well as to evaluate future potential therapeutic approaches, it is essential to have a highly reproducible model that displays long-term survival. Though a range of rodent models has been employed in the literature, there are questions regarding reproducibility, especially in terms of ischemic zone (i.e., degree of ischemia) and long-term survival. We have developed a highly reproducible stroke model that produces a consistent ischemic zone as a result of direct transient occlusion of the middle cerebral artery (MCA) in CB-17 (CB-17/Icr-+/+Jcl) mice. The model employs a thin monofilament to twist the artery resulting in complete interruption of blood flow. Transient ischemia can be induced for up to 240 min and the survival rate at 7 days post-ischemia was more than 60%, even in mice subjected to 240 min of transient ischemia resulting in hemorrhagic infarction in most animals. Our method can be used to model several pathologic conditions, such as reversible reperfusion injury, delayed neuronal death, necrotic brain injury and hemorrhagic infarction. We believe this preclinical model provides a step forward for testing future therapeutic approaches applicable to patients with ischemic brain injury.

1. Introduction

Cerebral reperfusion is known to be associated with serious brain injury, including enhanced oxidant stress/injury, hemorrhagic transformation and fatal edema. Various mechanisms, such as increased production of free radicals (Chan, 1996), disruption of the blood–brain barrier (BBB) (del Zoppo and Mabuchi, 2003), overload of critical cells with calcium ions, leukocyte accumulation in ischemic vasculature (del Zoppo et al., 1991), and subsequent infiltration of the brain parenchyma (Zhang et al., 1994), are involved in reperfusion injury. The impact of each process on cerebral injury often varies with the length and degree of ischemia. In order to simulate ischemia/reperfusion associated in clinical stroke, a highly reproducible model with long-term survival is required.

Many rodent stroke models employ an intraluminal suture for experimental ischemia/reperfusion. The latter model has the advantage of not requiring a craniotomy. However, insertion of a suture into the carotid artery interrupts blood flow to a wide territory including that of the ipsilateral MCA area, and also reduces blood flow to the ipsilateral posterior cerebral artery (PCA) and anterior cerebral artery (ACA) area, where the contralateral artery provides perfusion at a range of levels via the circle of Willis. These issues probably underlie the diminished reproducibility of the ischemic area and long-time survival in this model (Kitagawa et al., 1998; Kanemitsu et al., 2002).

Recently, we have found that the cerebral vasculature of CB-17 mice is identical comparing many animals. We have previously demonstrated that direct electrocoagulation of the M1 distal portion of the MCA in CB-17 mice induces highly reproducible and selective cortical infarction with high survival rates for extended periods (Taguchi et al., 2010). Transient ischemia can be induced by a modification of this permanent ischemia protocol (Kasahara et al., 2012). In the current manuscript, we provide detailed methods for such a new model of transient ischemia in CB-17 mice, allowing for easy replication of our work, and discuss the advantages and limitations of our model.

2. Materials and methods

All procedures were performed under auspices of an approved protocol from the Institute of Biomedical Research and Innovation Animal Care and Use Committee.

* Corresponding author at: Department of Regenerative Medicine Research, Institute of Biomedical Research and Innovation, 2-2 Minatojima-Minamimachi, Chuo-ku, Kobe 650-0047, Japan. Tel.: +81 78 304 5772; fax: +81 78 304 5263.
E-mail address: taguchi@fbri.org (A. Taguchi).

0168-0102/$ – see front matter © 2013 Elsevier Ireland Ltd and the Japan Neuroscience Society. All rights reserved.
http://dx.doi.org/10.1016/j.neures.2013.04.001

2.1. Induction of transient focal cerebral ischemia with craniotomy

Male CB-17 (CB-17/Icr-+/+Jcl) mice were purchased from Clea Japan (Tokyo, Japan). Mice were used at 7 weeks of age at weights of 22–26 g. Animals were allowed access to food and tap water ad libitum. Powdered chow and sterilized water were also provided during the first 7 days after induction of stroke.

Transient MCA occlusion was induced according to our modification of the Tamura method as described (Taguchi et al., 2010; Tamura et al., 1981). In brief, general anesthesia was induced and maintained by inhalation of 3% and 1.5% halothane (7025 Rodent Ventilator, Ugo Basile, Italy), respectively. Mice were placed in a lateral position, and a skin incision was made at the midpoint between the left orbit and the external auditory canal (Fig. 1A). Under an operating microscope (KOM300S, Konan Medical, Nishinomiya, Japan), the upper part of the temporalis muscle was pushed aside after partial resection of the left zygoma to allow visualization of the MCA through the cranial bone. A 1- to 2-mm burr hole was made using a dental drill (C710, Senko Medical Instrument Manufacturing, Tokyo, Japan), and the dura matter was opened and retracted cautiously so as not to damage the surface of the brain. Then, the MCA was isolated (Fig. 1B, lower magnification; C, higher magnification) and transiently occluded with a monofilament nylon suture distal to crossing the olfactory tract (distal M1 portion, Fig. 1D). A 2-mm length of 7–0 monofilament nylon suture (Tyco, USA), with the tip bent into a hook, was passed under the distal portion of the MCA. Subsequently, both ends of the suture were picked up and rotated 180 degrees clockwise horizontally with artery (Fig. 1E). It is notable that 7–0 nylon suture is stiffer than the artery, thus, rotation of the suture with the artery does not twist the suture but loops the artery around the suture resulting in complete interruption of blood flow (Fig. 1F). Mice were returned to cages in a controlled environment at 35–37 °C, where they were kept until reperfusion without anesthesia. After occlusion for 15, 20, 25, 120, 180, 240, 300 or 360 min, mice were placed again under anesthesia, and MCA blood flow was restored by putting the nylon suture back in place by counterclockwise rotation (Fig. 1G). During surgery, rectal temperature was monitored and controlled at 37.0 ± 0.2 °C by a feedback-regulated heating pad (ATB-1100, Nipponko-den, Tokyo, Japan). Cerebral blood flow (CBF) in the MCA area was monitored as described (Taguchi et al., 2004). Briefly, an acrylate column (Neuroscience Co., Ltd., Osaka, Japan) was attached to the intact skull using stereotactic coordinates (1 mm anterior and 3 mm lateral to the bregma), and CBF was monitored using a linear probe (1 mm in diameter) by one-dimensional laser Doppler flowmetry (Neuroscience Co., Ltd.).

2.2. Evaluation of stroke volume

At 24 and 48 h after induction of transient ischemia, mice brains were removed and sectioned coronally (1 mm thick) ($N = 8$ in each group). To evaluate the viability of brain tissue, coronal sections were incubated in 1% 2,3,5-triphenyltetrazolium (TTC: Sigma–Aldrich, St. Louis, MO) for 20 min at 37 °C in the dark and fixed in 4% paraformaldehyde/phosphate-buffered saline (PBS; pH 7.4). Infarct volume was measured using a microscopic digital camera system (Olympus, Tokyo, Japan). The TTC-positive area of each hemisphere was estimated using National Institutes of Health Image software (Version 1.62), and volume of the surviving/viable tissue was calculated by integrating the overall coronal-oriented area. Percent stroke volume was evaluated by [(contralateral hemisphere volume) − (infarcted hemisphere volume)]/[(contralateral hemisphere volume) × 2] × 100%, as described (Kasahara et al., 2012). In studies to evaluate long-term survival, 16 mice were used in each group.

2.3. Visualization of cerebral blood flow by laser speckle flowmetry

Cerebral blood flow (CBF) in the MCA area was visualized by laser speckle flowmetry (Omegazone laser speckle blood flow imager, Omegawave, Inc., Tokyo, Japan), as described previously ($N = 4$ in each group) (Nakano-Doi et al., 2010). In brief, the animal's skull was exposed and illuminated by a 780 nm semiconductor laser light. Twenty minutes of transient ischemia was induced and CBF of the same mice was sequentially evaluated at the following time points; before MCA occlusion (pre-MCAO), soon after MCA occlusion (MCAO), just before reperfusion (0 min), 5 and 60 min after reperfusion. To quantify cerebral blood flow, the region of interest (ROI) was positioned at 2.5 mm dorsal and 3 mm lateral from the bregma (i.e. the ischemic core region of MCA territory). The same grid was used to set the matching region on the contralateral side. The ratio of CBF was calculated by [(ipsilateral cerebral blood-flow)/(contralateral cerebral blood-flow)].

2.4. Data analysis

In all experiments, mean ± standard deviation is reported. JMP 8.02 (SAS Institute Inc., Co., NC, USA) was used for statistical analysis.

3. Result

3.1. Reproducible transient ischemia can be inducible up to 240 min

In a previous report, we have demonstrated a reproducible murine model of permanent cerebral ischemia by electrocoagulation of the distal portion of the MCA in CB-17 mice (Taguchi et al., 2010). In this study, we have modified the latter technique to develop a reproducible model of cerebral reperfusion injury.

All mice showed >70% decrease in cerebral blood flow rapidly after occlusion and all mice showed >80% restored cerebral blood flow soon after release of the occlusion (after 15, 20, 25, 120, 180 or 240 min of transient ischemia), compared with before transient ligation of the MCA as evaluated by one-dimensional laser Doppler flowmetry. However, rapid and reproducible reperfusion was not observed in mice after 300 or 360 min transient ischemia. Thus, mice subject to 300 or 360 min of transient ischemia were not further studied.

To investigate neuronal death after transient ischemia, brain sections were stained with TTC at 24 h after transient ischemia (Fig. 2A). No TTC-negative cerebral cortex was observed in mice after 15 min of ischemia. Only a small TTC-negative area was observed in mice subjected to 20 min of ischemia. In contrast, highly reproducible cerebral infarction was observed in all mice after 25, 120, 180 or 240 min of transient ischemia, similar to what we observed previously in the permanent MCA occlusion model (Taguchi et al., 2010). At 48 h after ischemia (Fig. 2B), there was still no TTC-negative area in mice subjected to 15 min of ischemia. In contrast, an highly reproducible TTC-negative area was observed after 20 min of ischemia, similar to that seen in mice after 25, 120, 180 or 240 min of transient ischemia. It is notable that the TTC-negative area of all samples was strictly restricted to the cerebral cortex of the MCA territory and did not include the striatum. Mean % stroke volume of each sample at 24 and 48 h after ischemia is shown in Fig. 2C and D, respectively. To confirm survival of neuronal tissue after 15 min of transient ischemia, brain sections in mice subjected to 15 min of ischemia were investigated at 7 days

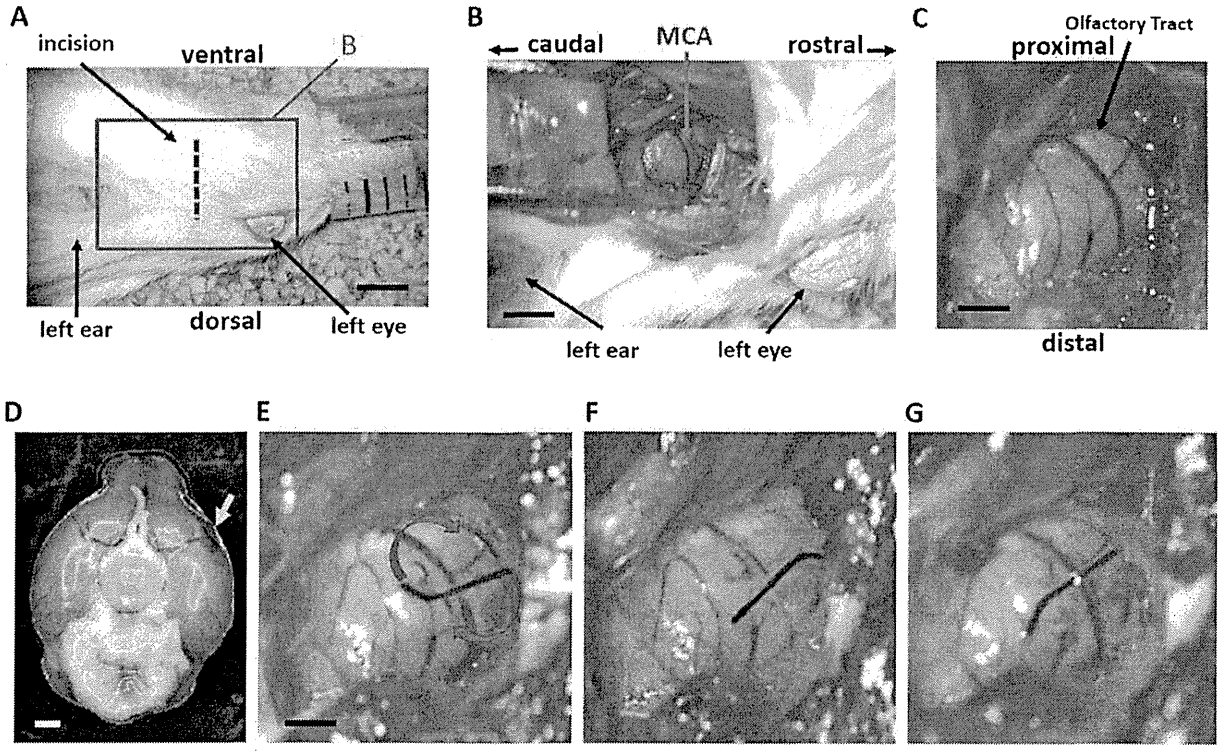

Fig. 1. Direct occlusion of the MCA followed by reperfusion. (A) Orientation of mice for induction of ischemic/reperfusion. The blue rectangle represents the enlarged area shown in panel B. (B, C) After partial resection of the left zygoma, a burr hole was made and the dura matter removed to allow isolation of the MCA (B, lower magnification; C, higher magnification). (D–F) The distal M1 portion of the MCA in CB-17 mice was directly occluded with a nylon monofilament. The arrow indicates the distal M1 portion of MCA in CB-17 mice (D). The suture was passed under the MCA and rotated 180° clockwise around the MCA (E). (F, G). Blood-flow in the distal portion of MCA was completely blocked (F). After ischemia, blood flow in the MCA was restored by putting the monofilament back into the original position (G). Scale bars, 5 mm (A), 2 mm (B), 0.6 mm (C, E) and 1.5 cm (D).

after ischemia. In the latter case, no TTC-negative area was found (not shown).

3.2. *Ischemic period and hemorrhagic transformation*

Hemorrhagic transformation is a life-threatening event complicating thrombolytic and/or vascular interventional therapy. Development of novel treatments to prevent hemorrhagic transformation is highly desirable for safer thrombolytic therapy that might also provide a longer therapeutic time window. Thus, using our model, at 24 h after reperfusion, the incidence and the severity of hemorrhagic infarction were investigated. Though no hemorrhagic infarction was observed in mice after ≤25 min ischemia, 90% of mice subjected to 240 min of ischemia showed hemorrhagic infarction in the MCA area (Fig. 2A and B arrow head). The incidence of hemorrhagic infarction is shown in Fig. 2E.

3.3. *Ischemic period and long-term survival rate*

To evaluate the therapeutic potential of novel treatments on ischemia/reperfusion injury, it is essential to investigate the outcome over longer periods (up to a week) rather than just hours after the ischemic insult. Using the intraluminal suture method, the degree of ischemia varies between areas. Thus, prolongation of the ischemic period has always been linked to variable/nonreproducible expansion of the stroke area and often results in a low survival rate during the chronic period (Memezawa et al., 1992; Popp et al., 2009). In contrast, in the current model, stroke area appears to be consistently restricted to the cerebral cortex of MCA area regardless of the period of ischemia. Fig. 3 shows survival on day 1, 3, 5 and 7 after transient ischemia. It is notable that the survival rate in mice subjected to 240 min of ischemia, where 90% of mice show hemorrhagic infarction, was more than 60% at day 7.

3.4. *Temporal changes of cerebral blood flow*

Two-dimensional laser speckle flowmetry analysis was employed to visualize temporal changes of cerebral blood flow (Fig. 4A–E). The decreased level of cerebral blood flow was maintained throughout the ischemic period and restored to more than 90% of the initial baseline by 5 min after the onset of reperfusion (Fig. 4F). At 60 min after reperfusion, the level of cerebral blood flow returned to that observed before MCA occlusion.

4. Discussion

In this article, we have described a highly reproducible cerebral ischemia/reperfusion model induced by direct temporal occlusion of MCA in CB-17 mice by twisting the artery using a thin monofilament. The duration of transient ischemia can be extended up to 240 min while maintaining a high survival rate at day 7 after reperfusion.

In previous studies, models of direct transient occlusion of the MCA have been described, such as those employing a micro-clip or a suture to occlude the MCA (Matsui et al., 1997; Shigeno et al., 1985). However, these models most often result in only incomplete occlusion/recirculation (Shigeno et al., 1985), and demand a very high level of surgical skill, especially in mice. Consequently, such models have gradually become less popular since the emergence of the intraluminal technique of transient MCA occlusion (Longa et al.,